Università degli Studi di Padova

Dipartimento di Geoscienze

Tesi di Laurea triennale in Scienze Geologiche

Anno accademico 2013-2014

STUDY OF "BULGED CRATERS" IN ARABIA TERRA (MARS)

Supervisor: Dr. Massironi Matteo

Co-supervisor: Dr. Pozzobon Riccardo

Bachelor-Degree candidate: Giovanni Baldo

What's a bulge?

A bulged crater is carachterized by a central swelling in the crater's floor, unrelated to impact derived central peak.

The origin is widely debated and two possible causes has been proposed so far:

- Erosion by circolar blowing of winds within the crater (Andrews-Hanna et al. 2010, JGR)
- Sub-surface fluids effusions and accretion of spring material (Pondrelli et al. 2011, EPSL)

Our suggestion is that they are caused by uprising of evaporitic material through passive diapirism.

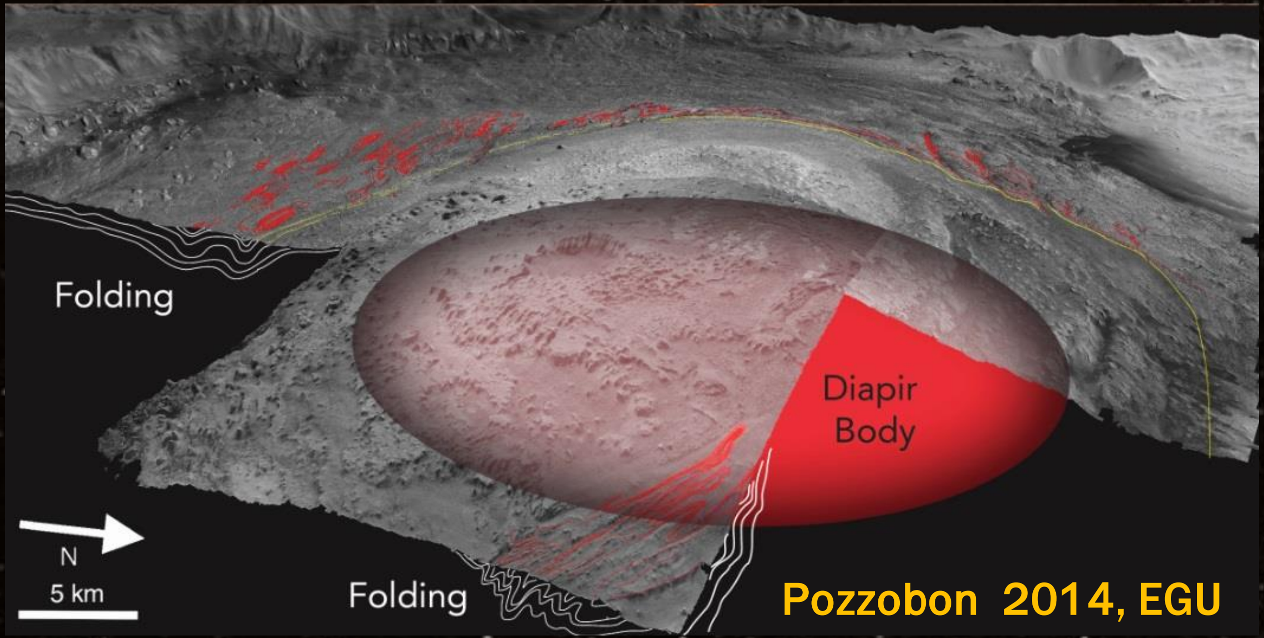

Arabia Terra area is suitable for bulged craters for the following reasons:

- high craters density with different sizes (highland);
- already reported bulged craters infilled by sedimentary deposits;
- gentle slope degrading towards the northern lowlands where sabka enviornments could have been favoured during the Noachian.

Arabia Terra

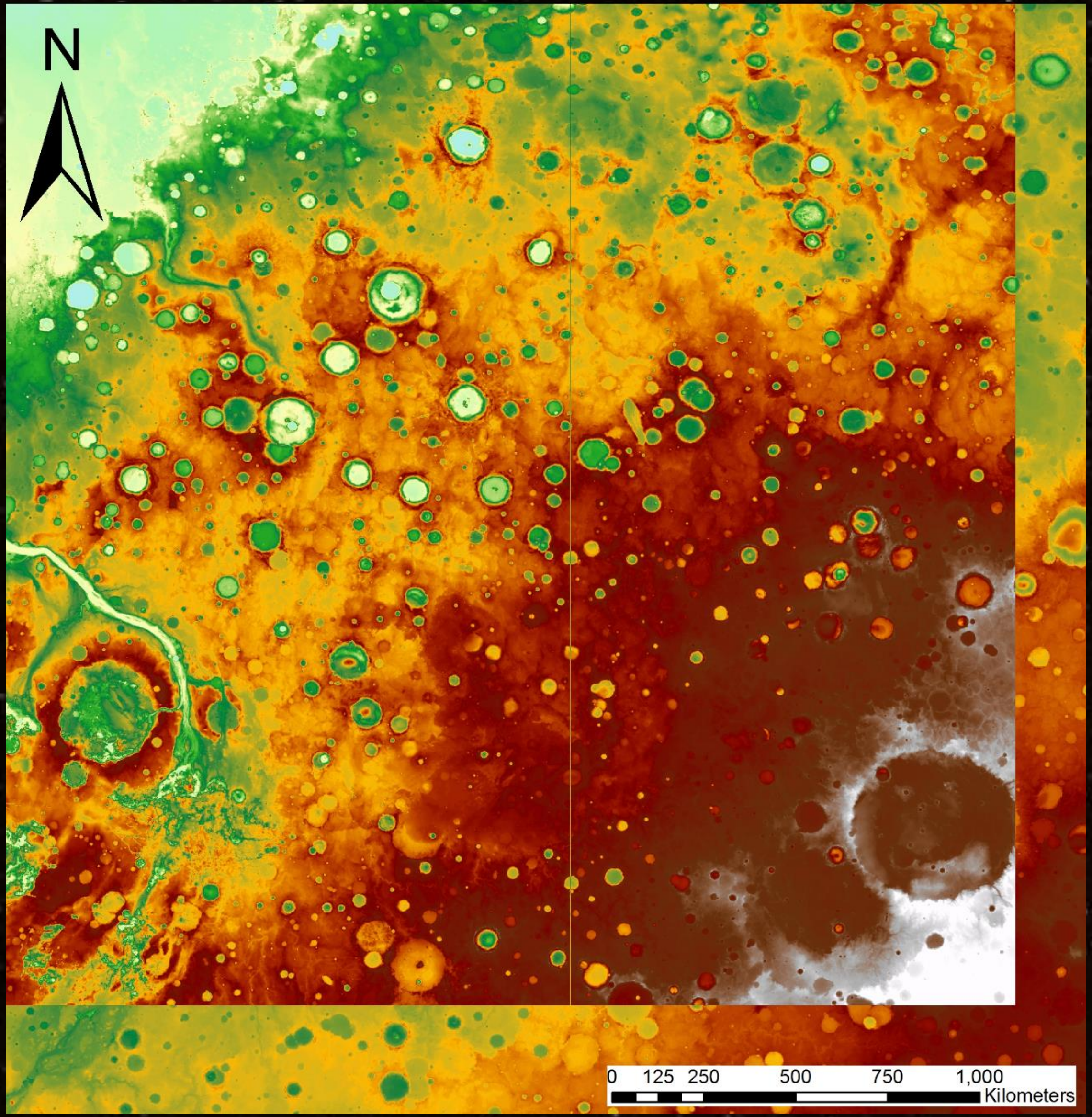

We operated in two different ways:

1) We have analyzed topographic profiles (MOLA 128px/deg) of all craters (larger than 15km in diameter) in an area of about 7’360’000km^2 to retrive shape and dimensions of possible inner bulges and to determine their distribution in Arabia Terra.

2) We created a geological map of a representative bulged crater to discover possible traces of other processes which could be hints of evaporitic uprising.

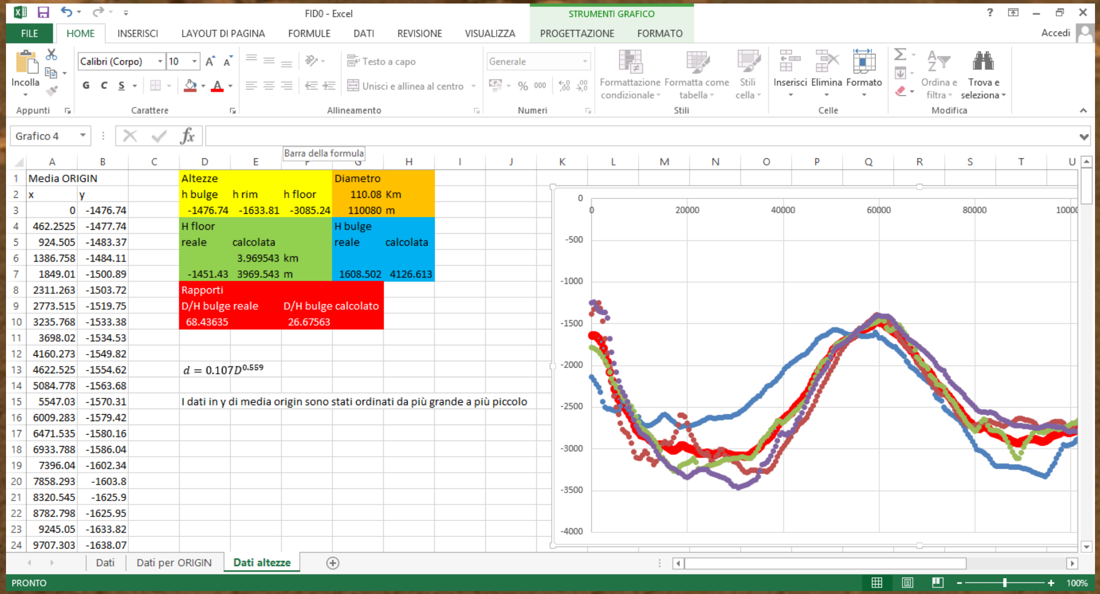

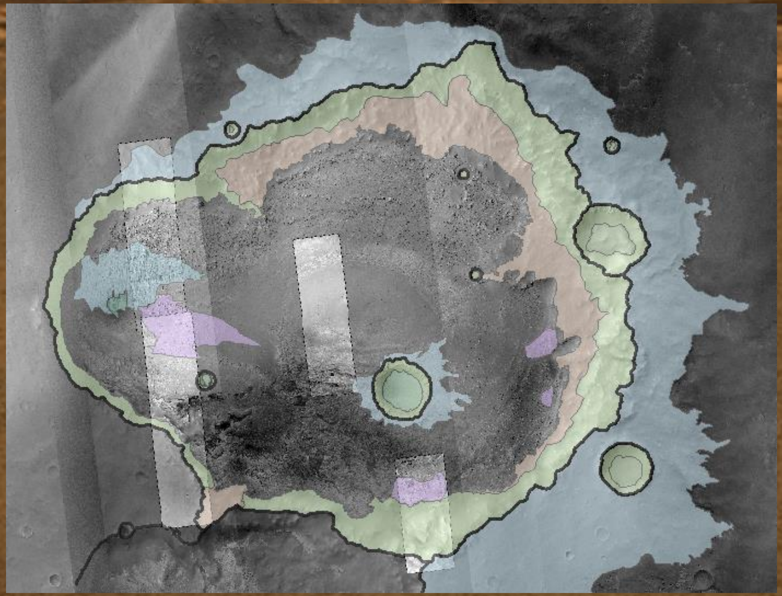

Phase 1: craters topographic profiles analyses

Data:

- MOLA topographic (128px/deg)
- THEMIS IR day (512 m/px)
- HRSC DTM (50 m/px)
- CTX mosaic (6 m/px)
- Robbins craters database (2012, JGR)

Software:

- ISIS3
- ArcCatalog
- ArcMap
- Excel
- Origin
- MathLab
- Paint.NET

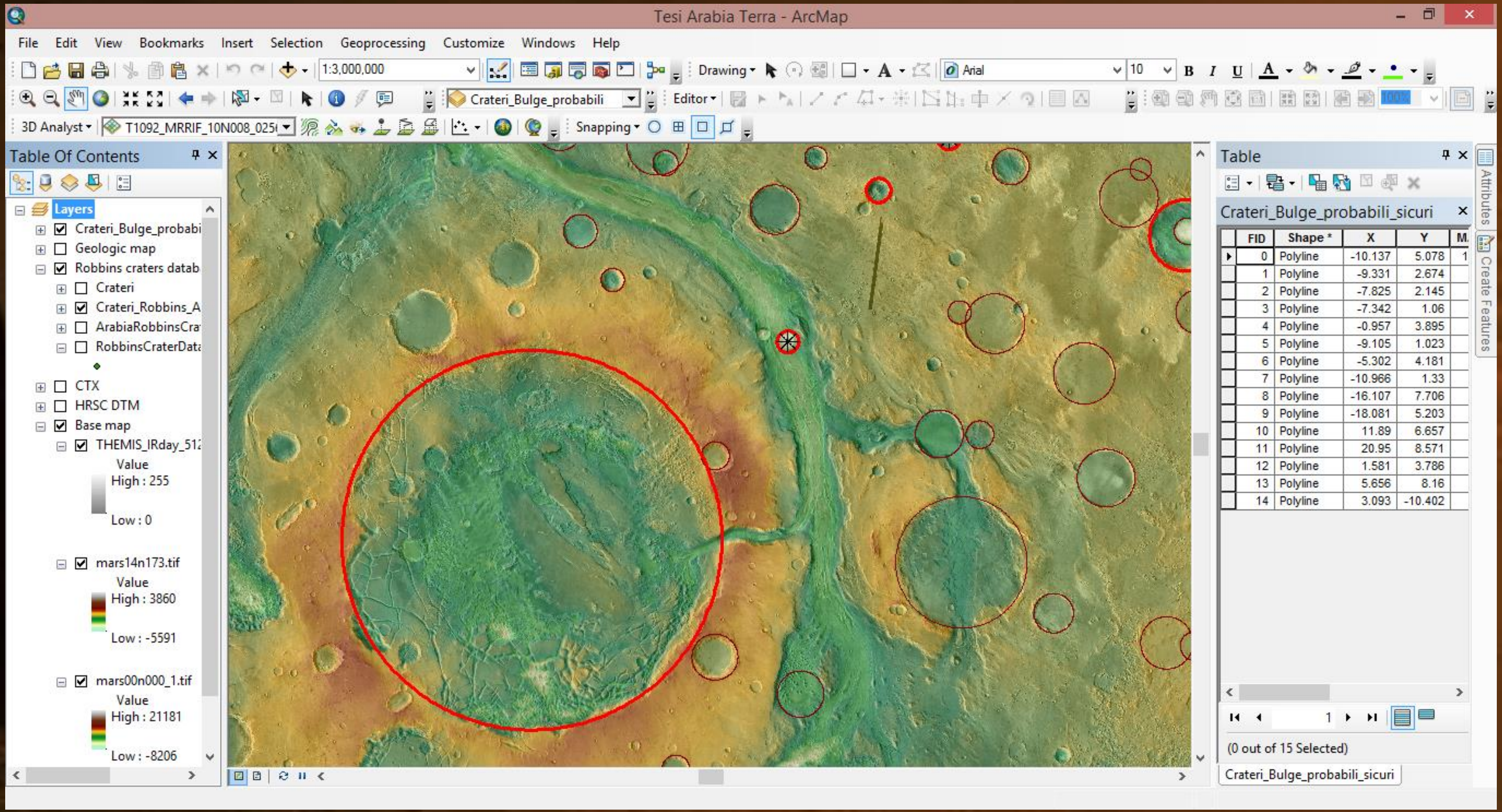

Step 1: detection of bulged craters in Arabia Terra

Robbins craters database

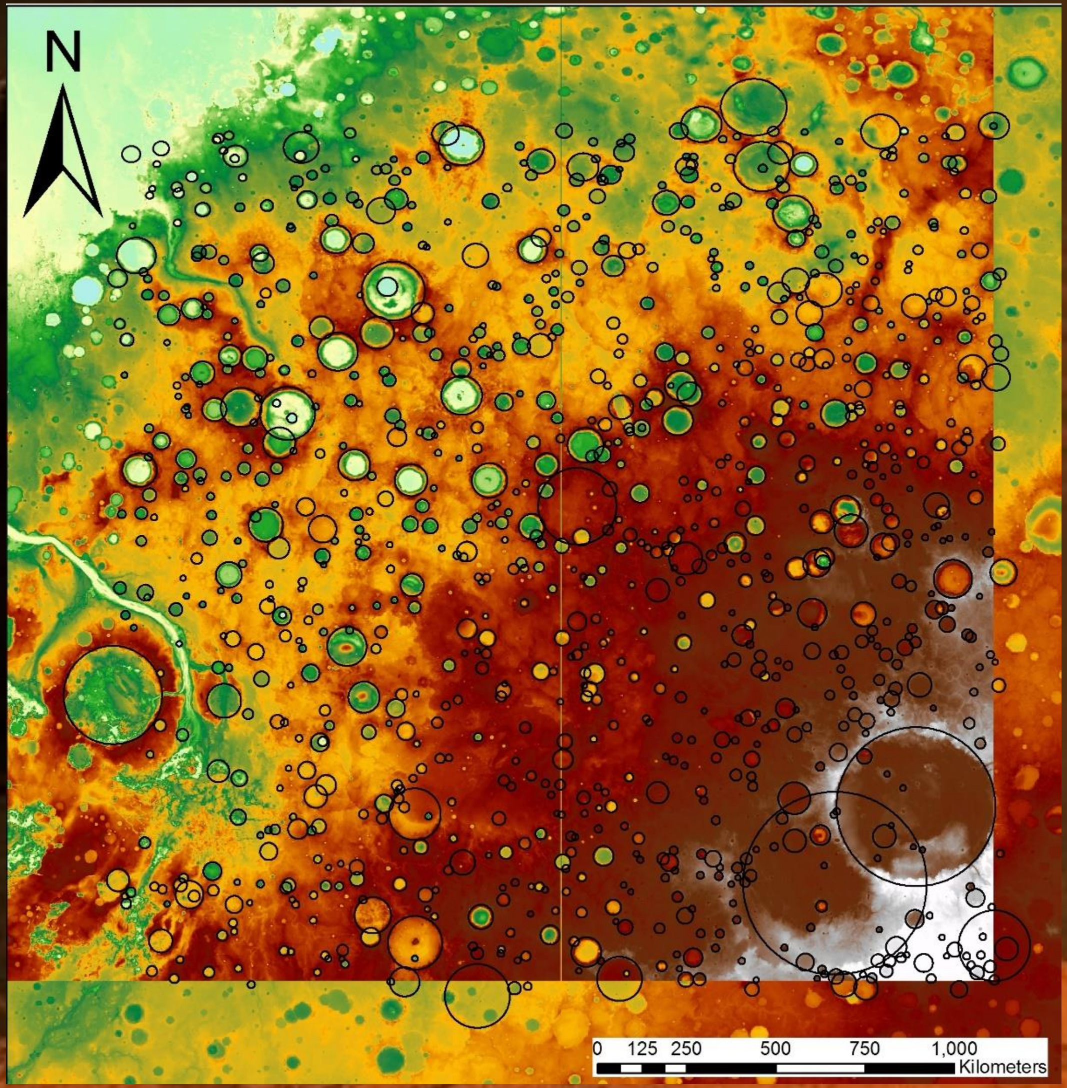

Step 1: detection of bulged craters in Arabia Terra

Probable bulged craters

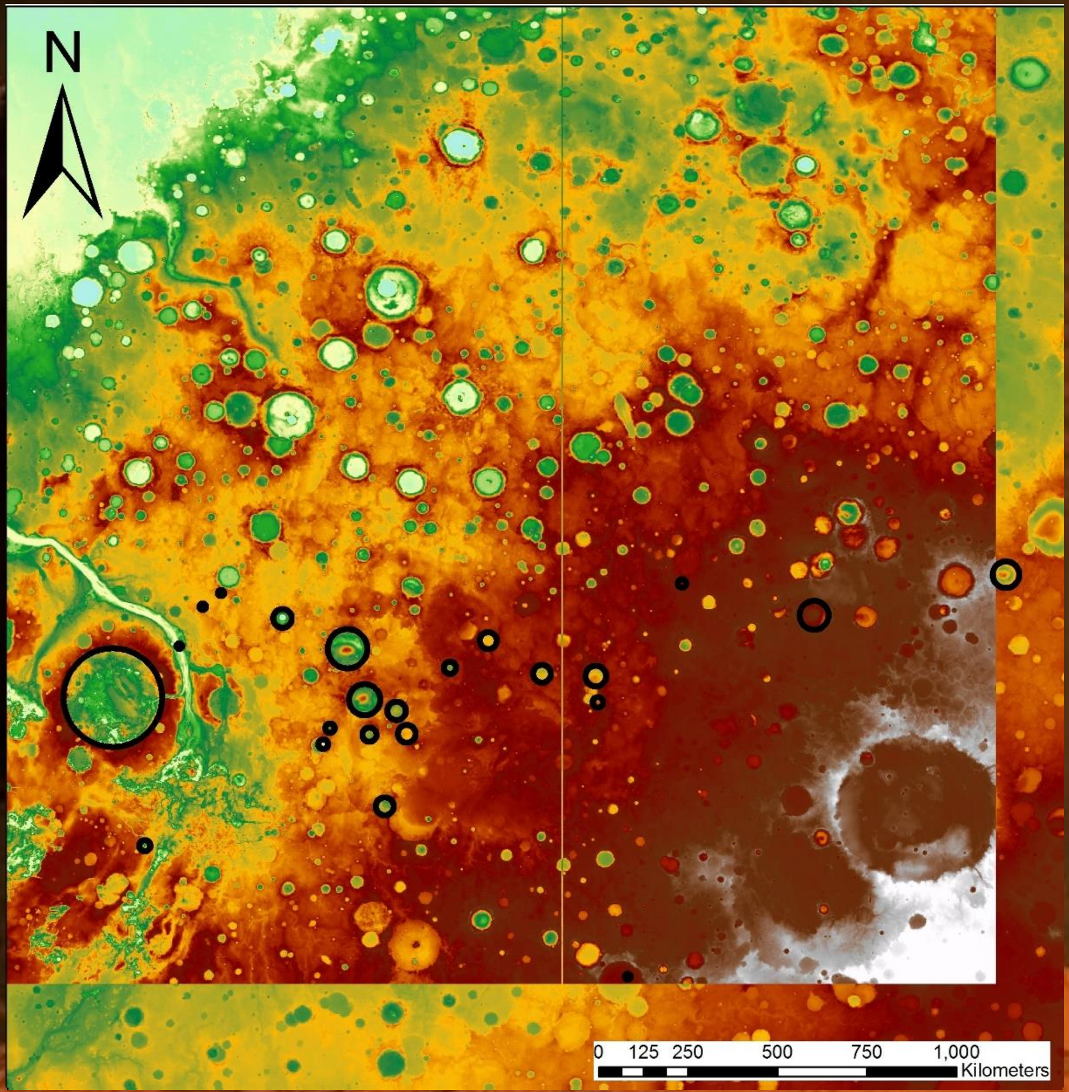

Step 1: detection of bulged craters in Arabia Terra

Ambiguous bulged craters

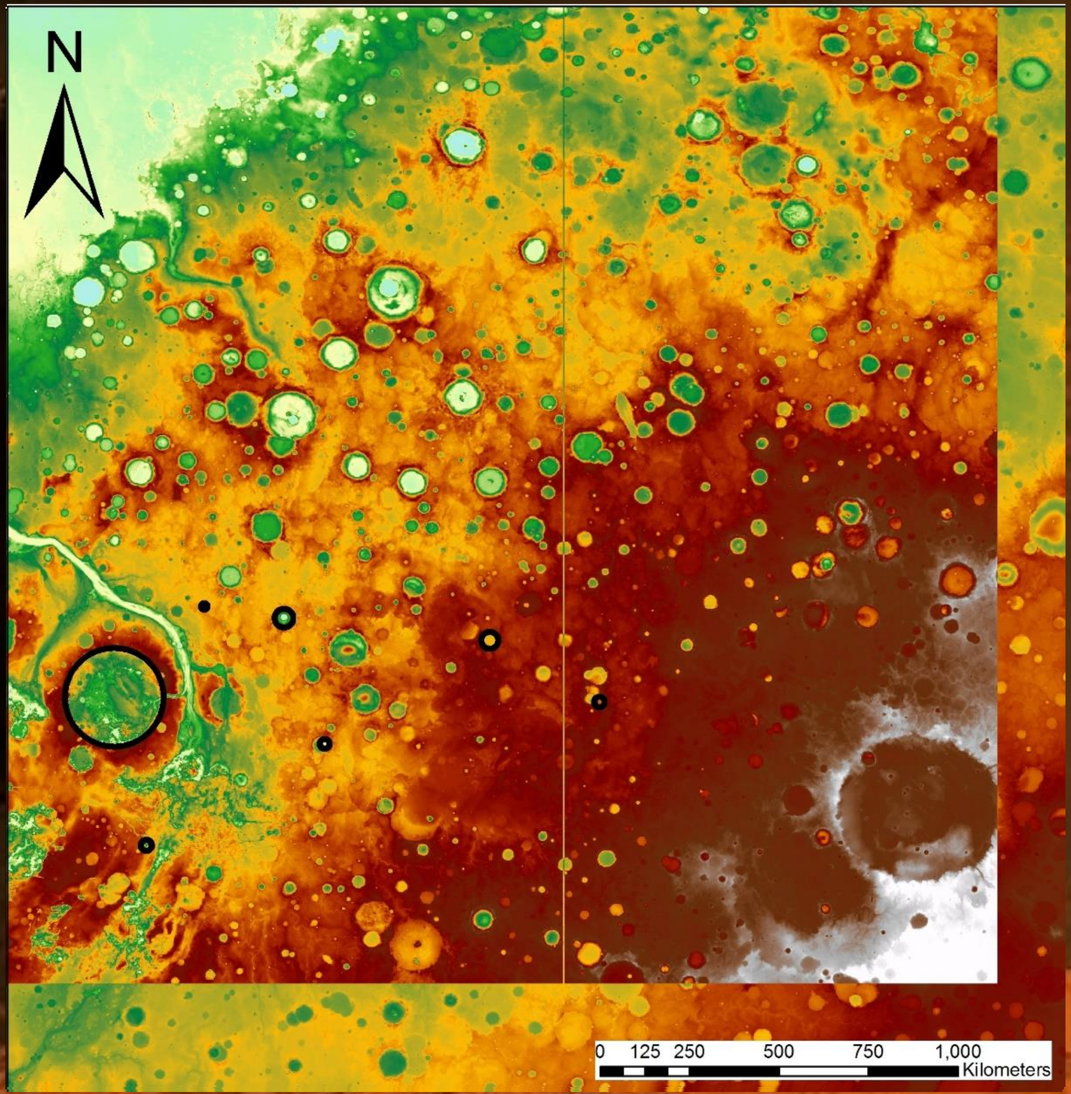

Step 1: detection of bulged craters in Arabia Terra

Craters with chaotic inner infilling

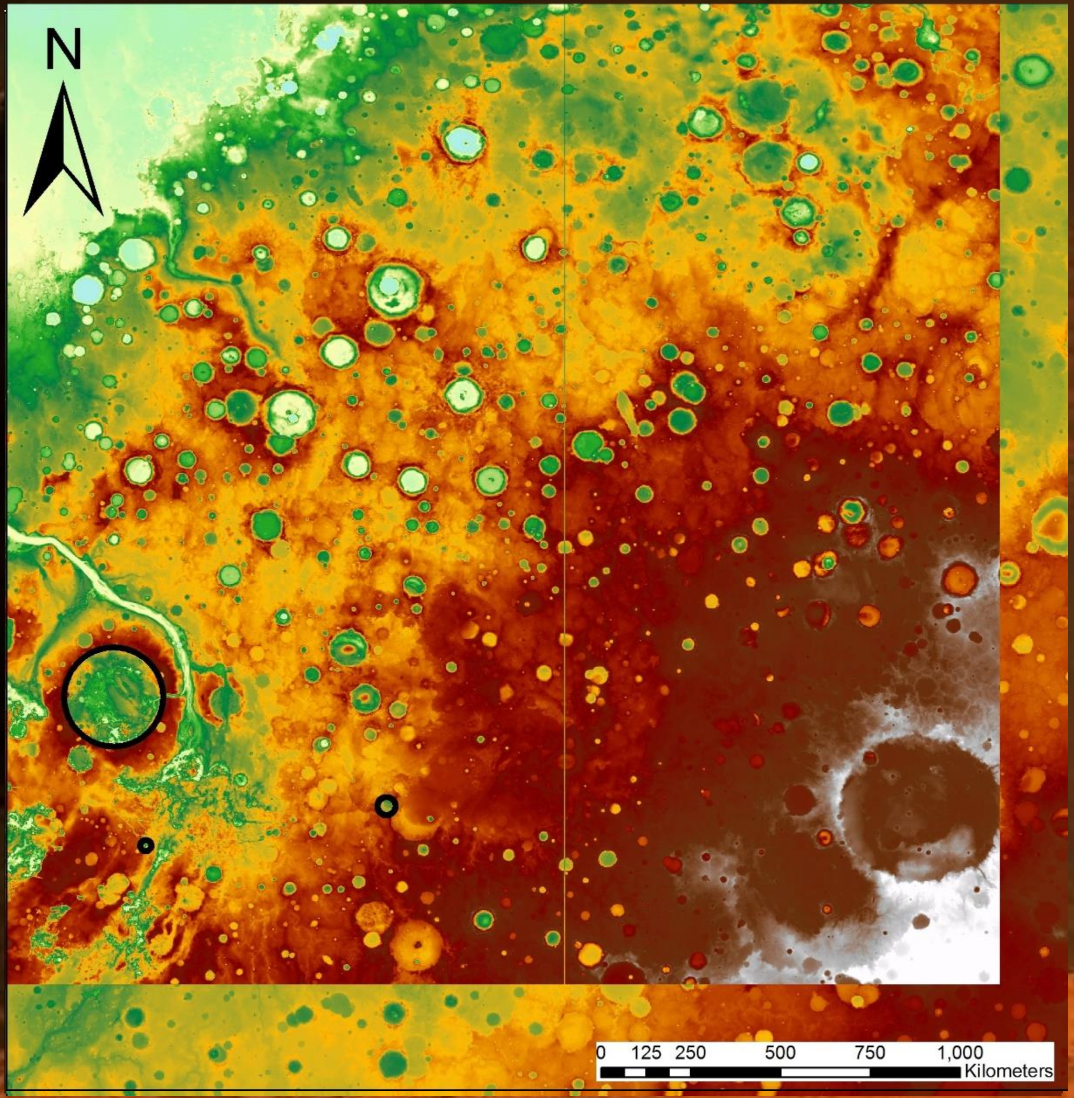

Step 1: detection of bulged craters in Arabia Terra

Bulged craters for sure

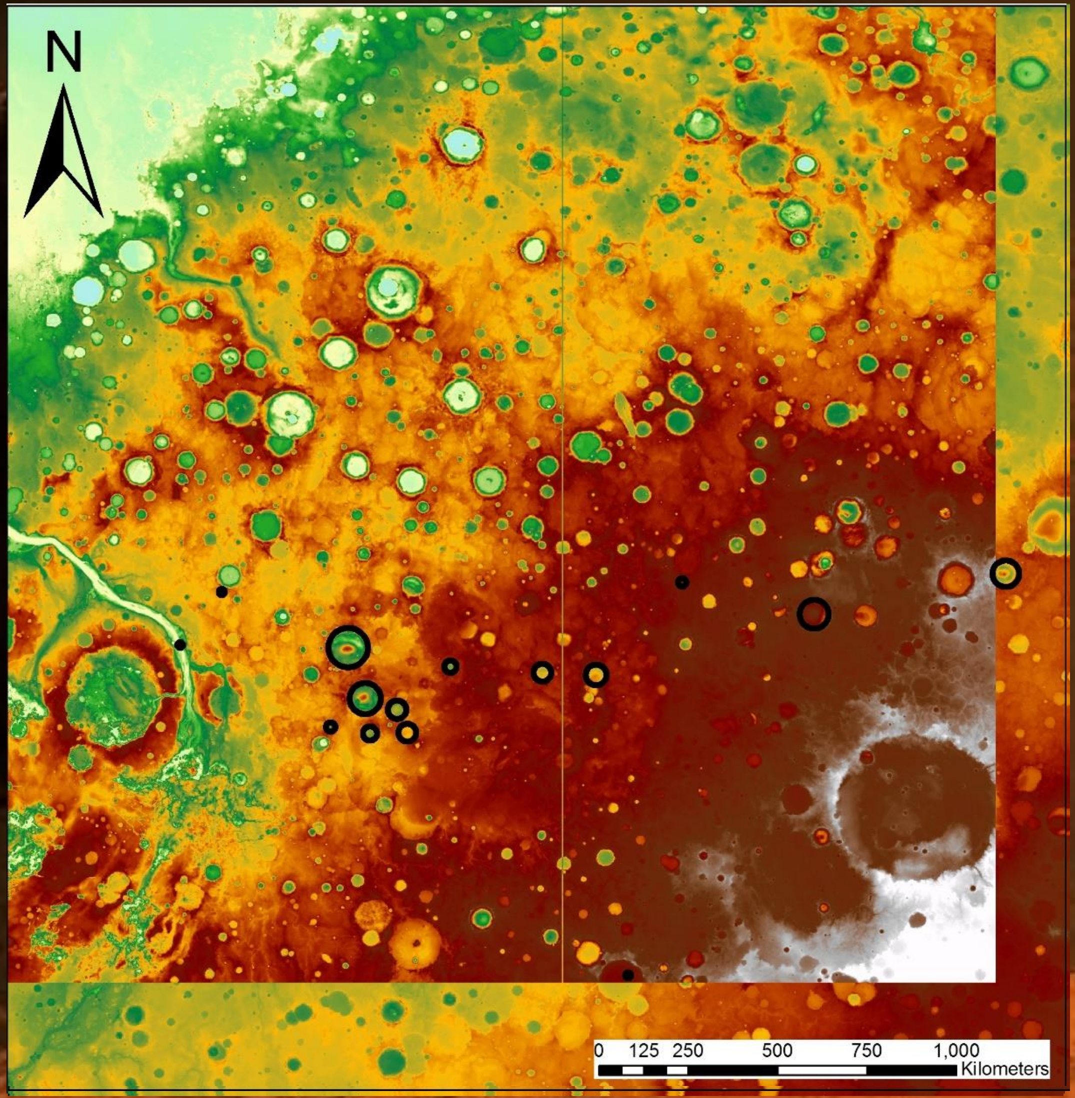

Step 2: topographic profiles of sure bulged craters

For each sure crater we have drawn four topographic profiles.

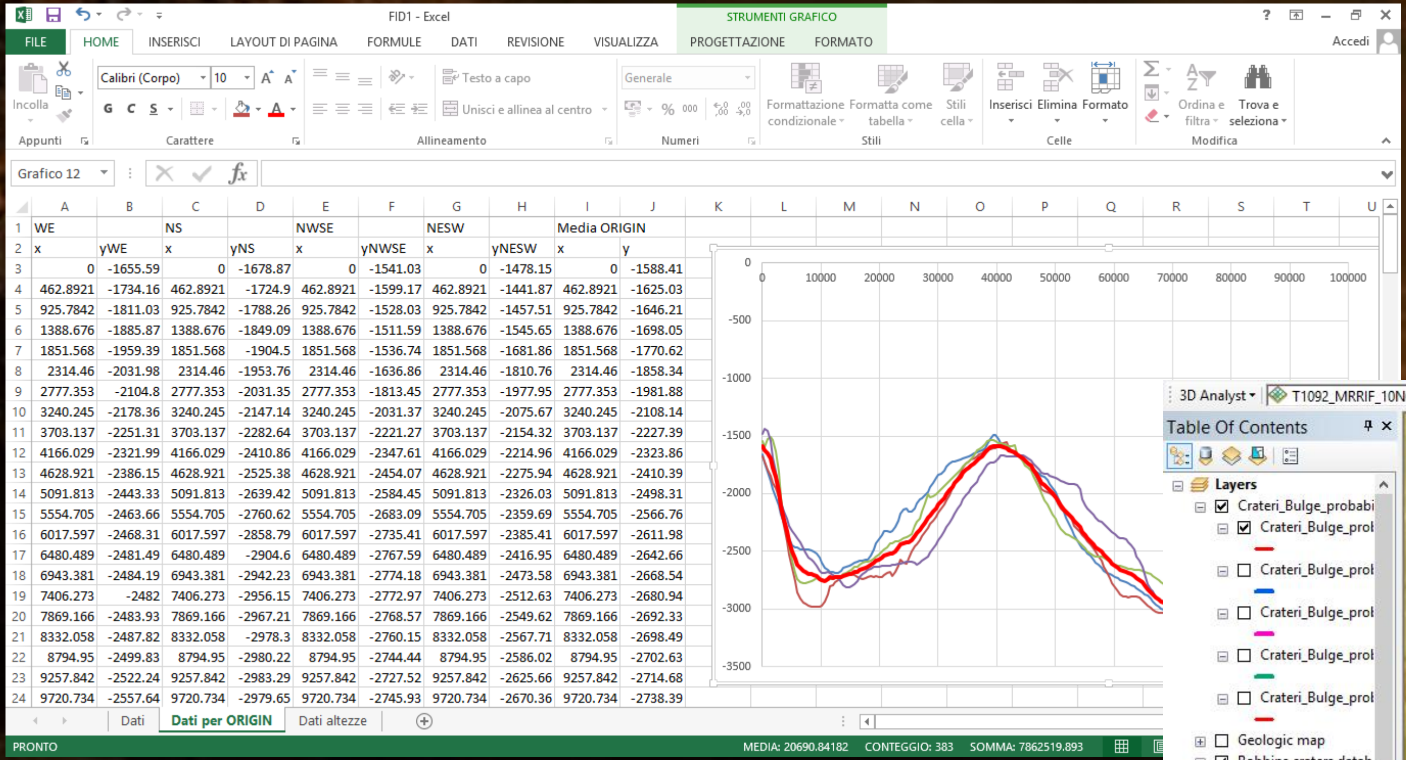

WE		NS		NWSE		NESW		Media ORIGIN	
x	yWE	x	yNS	x	yNWSE	x	yNESW	x	y
0	-1655.59	0	-1678.87	0	-1541.03	0	-1478.15	0	-1588.41
462.8921	-1734.16	462.8921	-1724.9	462.8921	-1599.17	462.8921	-1441.87	462.8921	-1625.03
925.7842	-1811.03	925.7842	-1788.26	925.7842	-1528.03	925.7842	-1457.51	925.7842	-1646.21
1388.676	-1885.87	1388.676	-1849.09	1388.676	-1511.59	1388.676	-1545.65	1388.676	-1698.05
1851.568	-1959.39	1851.568	-1904.5	1851.568	-1536.74	1851.568	-1681.86	1851.568	-1770.62
2314.46	-2031.98	2314.46	-1953.76	2314.46	-1636.86	2314.46	-1810.76	2314.46	-1858.34
2777.353	-2104.8	2777.353	-2031.35	2777.353	-1813.45	2777.353	-1977.95	2777.353	-1981.88
3240.245	-2178.36	3240.245	-2147.14	3240.245	-2031.37	3240.245	-2075.67	3240.245	-2108.14
3703.137	-2251.31	3703.137	-2282.64	3703.137	-2221.27	3703.137	-2154.32	3703.137	-2227.39
4166.029	-2321.99	4166.029	-2410.86	4166.029	-2347.61	4166.029	-2214.96	4166.029	-2323.86
4628.921	-2386.15	4628.921	-2525.38	4628.921	-2454.07	4628.921	-2275.94	4628.921	-2410.39
5091.813	-2443.33	5091.813	-2639.42	5091.813	-2584.45	5091.813	-2326.03	5091.813	-2498.31
5554.705	-2463.66	5554.705	-2760.62	5554.705	-2683.09	5554.705	-2359.69	5554.705	-2566.76
6017.597	-2468.31	6017.597	-2858.79	6017.597	-2735.41	6017.597	-2385.41	6017.597	-2611.98
6480.489	-2481.49	6480.489	-2904.6	6480.489	-2767.59	6480.489	-2416.95	6480.489	-2642.66
6943.381	-2484.19	6943.381	-2942.23	6943.381	-2774.18	6943.381	-2473.58	6943.381	-2668.54
7406.273	-2482	7406.273	-2956.15	7406.273	-2772.97	7406.273	-2512.63	7406.273	-2680.94
7869.166	-2483.93	7869.166	-2967.21	7869.166	-2768.57	7869.166	-2549.62	7869.166	-2692.33
8332.058	-2487.82	8332.058	-2978.3	8332.058	-2760.15	8332.058	-2567.71	8332.058	-2698.49
8794.95	-2499.83	8794.95	-2980.22	8794.95	-2744.44	8794.95	-2586.02	8794.95	-2702.63
9257.842	-2522.24	9257.842	-2983.29	9257.842	-2727.52	9257.842	-2625.66	9257.842	-2714.68
9720.734	-2557.64	9720.734	-2979.65	9720.734	-2745.93	9720.734	-2670.36	9720.734	-2738.39

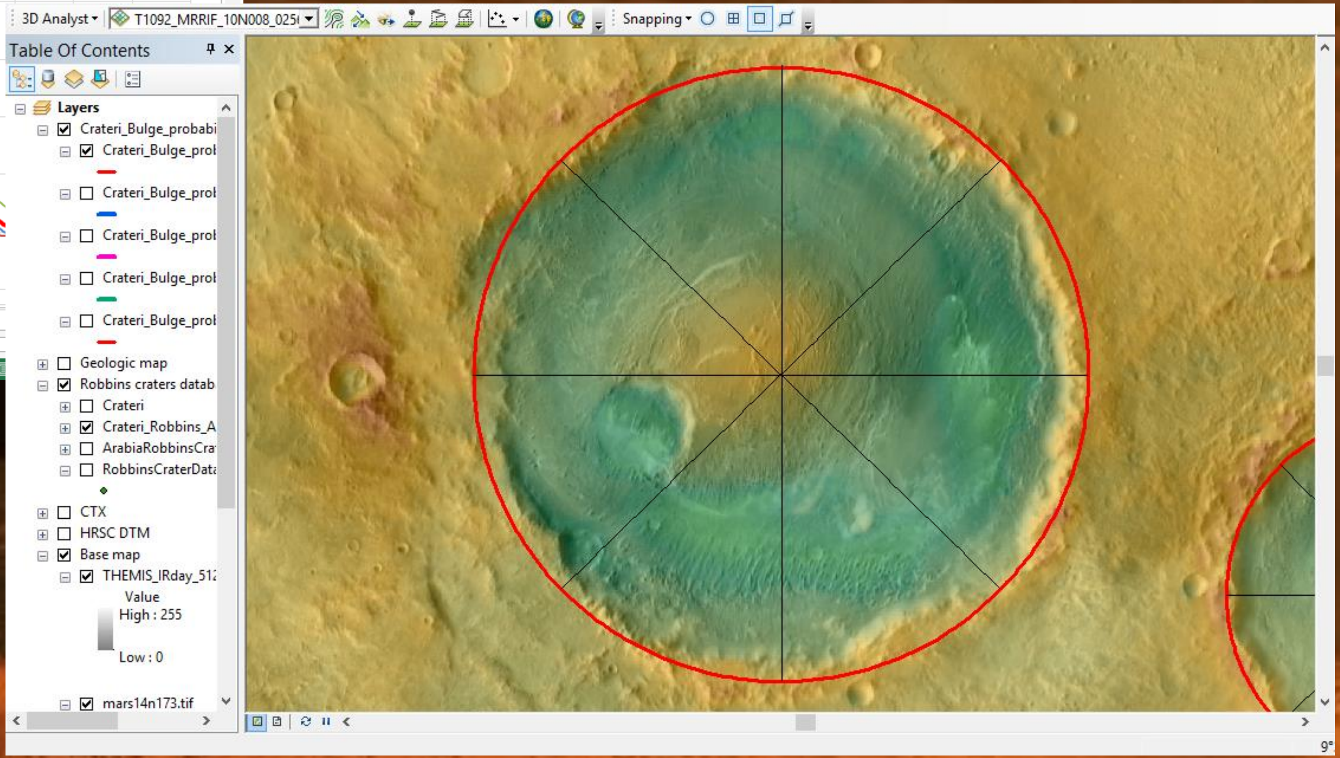

Then we used Origin to create a representative mean topographic profile for each crater.

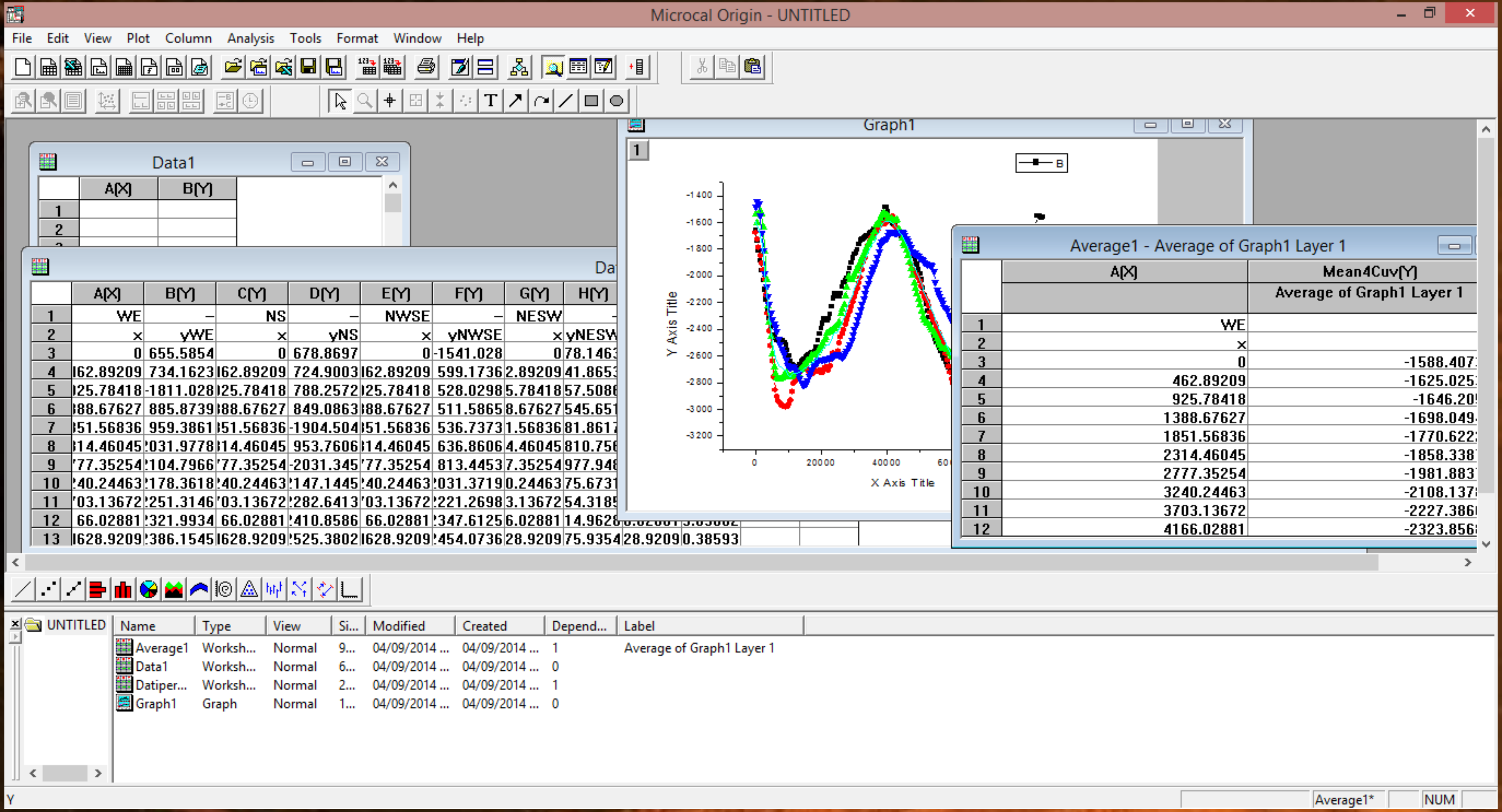

We have calculated the pristine depth of each bulged crater using Robbins equation for all global complex craters :

$$d=0.107D^{0.559}$$

where «d» stands for floor depth. (Robbins and Hynek 2012)

The pristine depth is different from real measured depth possibly for crater infilling.

ROBBINS AND HYNEK: MARS CRATER DATABASE—RESULTS

Table 2. Crater Depth/Diameter Ratios on Mars Over Different Terrains[a]

	Deepest Craters	Fresh Craters	All Craters
Global			
Smp (N = 37,091)	$d = 0.179D^{1.012}$	$d = 0.097D^{1.061}$	$d = 0.047D^{1.284}$
Cpx (N = 32,021)	$d = 0.286D^{0.582}$	$d = 0.250D^{0.527}$	$d = 0.107D^{0.559}$
−40° to +40°			
Smp (N = 24,875)	$d = 0.175D^{1.022}$	$d = 0.084D^{1.245}$	$d = 0.078D^{1.106}$
Cpx (N = 22,290)	$d = 0.280D^{0.570}$	$d = 0.229D^{0.567}$	$d = 0.155D^{0.464}$
≤−40°, ≥+40°			
Smp (N = 12,210):	$d = 0.177D^{0.724}$	$d = 0.083D^{1.073}$	$d = 0.014D^{1.465}$
Cpx (N = 9742)	$d = 0.244D^{0.579}$	$d = 0.174D^{0.629}$	$d = 0.032D^{0.881}$
Northern Plains			
Smp (N = 3693)	$d = 0.165D^{1.094}$	$d = 0.073D^{1.311}$	$d = 0.011D^{1.992}$
Cpx (N = 1308)	$d = 0.479D^{0.359}$	$d = 0.274D^{0.502}$	$d = 0.227D^{0.158}$
Volcanic Terrain			
Smp (N = 2471)	$d = 0.212D^{0.886}$	$d = 0.182D^{0.718}$	$d = 0.091D^{1.010}$
Cpx (N = 1008)	$d = 0.291D^{0.526}$	$d = 0.240D^{0.539}$	$d = 0.209D^{0.451}$
Southern Highlands			
Smp (N = 23,087)	$d = 0.235D^{0.777}$	$d = 0.154D^{0.821}$	$d = 0.051D^{1.261}$
Cpx (N = 23,850)	$d = 0.303D^{0.571}$	$d = 0.231D^{0.556}$	$d = 0.112D^{0.541}$
Polar Terrain			
Smp (N = 727)	-	-	$d = 0.0028D^{1.843}$
Cpx (N = 202)	-	-	$d = 0.014D^{1.161}$

[a]This table shows the simple (top line) and complex (bottom line) depth/Diameter relationship when they are divided into a variety of terrain types. The number N of craters in this table is the number used in the "All Craters" analysis.

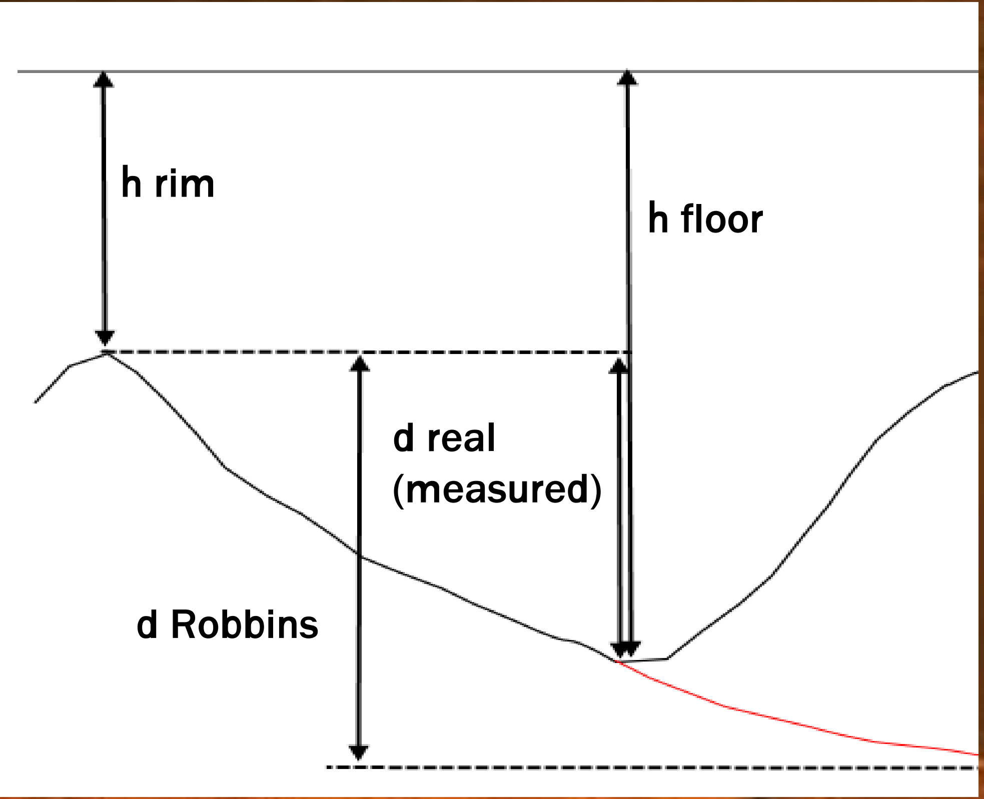

Similarly we have calculated the pristine elevation of the bulge and measured the real elevation.

Height			Diameter	
h bulge	h rim	h floor	87.34 Km	
-1588.75	-1588.41	-2996.74	87340 m	
H floor			H bulge	
real	calculated		real	calculated
	3.487897 Km			
-1408.33	3487.897 m		1407.99	3487.557
Relationship				
D/H bulge real		D/H bulge calculated		
62.03169		25.04332		

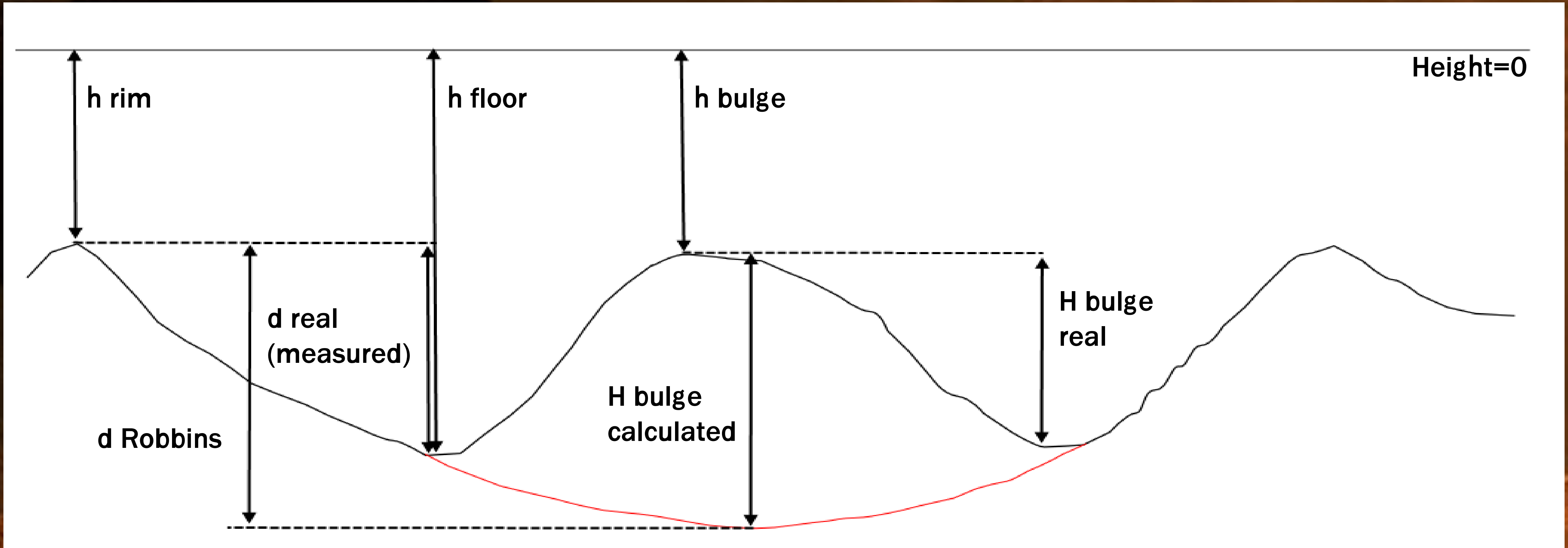

Step 3: results Best Fit measured diameter/height

Fit name: h_real
X data: D
Y data: h_real
Z data: (none)
Weights: (none)

Power
Number of terms: 1
Equation: a*x^b
Fit Options...

Auto fit
Fit
Stop

Results

General model Power1:
f(x) = a*x^b
Coefficients (with 95% confidence bounds):
a = 6.352e-008 (-4.837e-007, 6.107e-007)
b = 2.074 (1.319, 2.829)

Goodness of fit:
SSE: 6.912e+005
R-square: 0.8416
Adjusted R-square: 0.8294
RMSE: 230.6

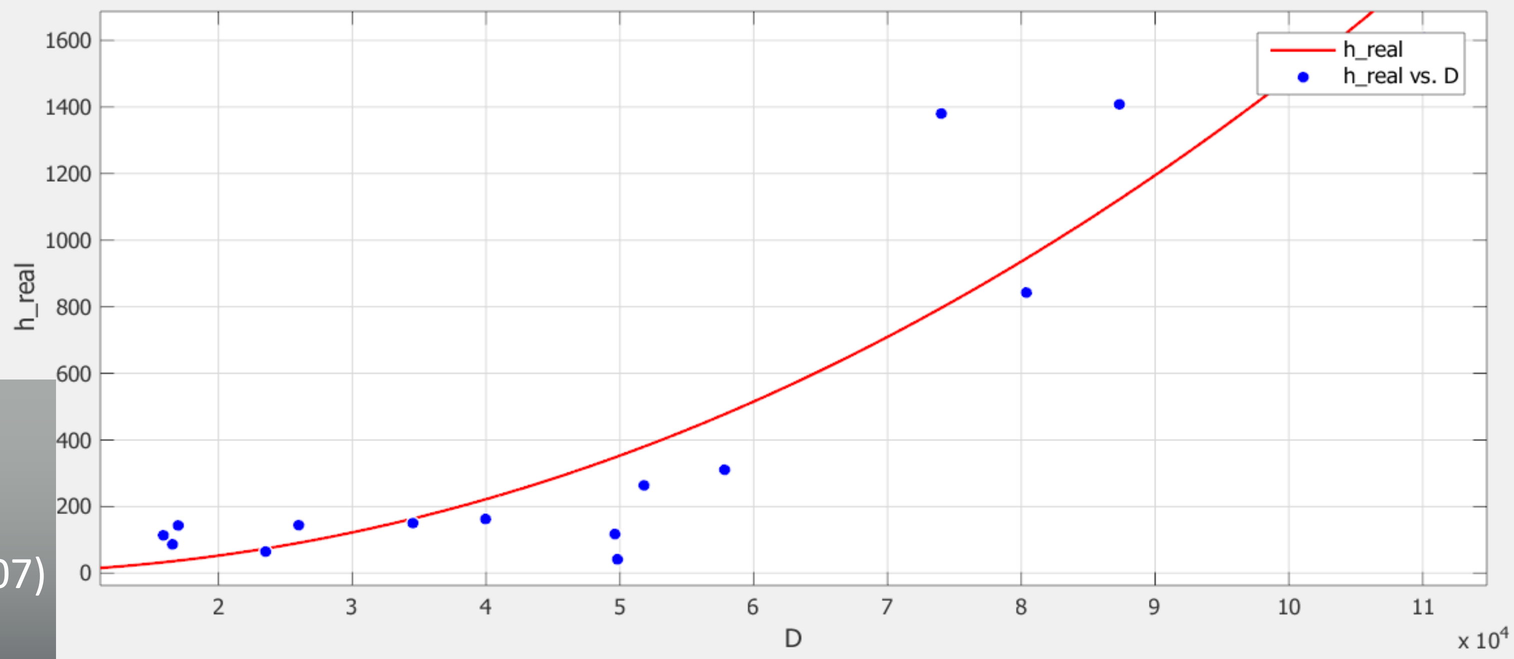

DFE	Adj R-sq	RMSE	# Coeff	Validation Data	Validation SSE	Validation RMSE
13	0.9388	286.8926	2			
13	0.8294	230.5922	2			

General model Power1:
f(x) = a*x^b
Coefficients (with 95% confidence bounds):
a = 6.352e-008 (-4.837e-007, 6.107e-007)
b = 2.074 (1.319, 2.829)

Goodness of fit:
R-square: 0.8416

…it seems to be an exponential trend

Step 3: results

Best Fit calculated diameter/height

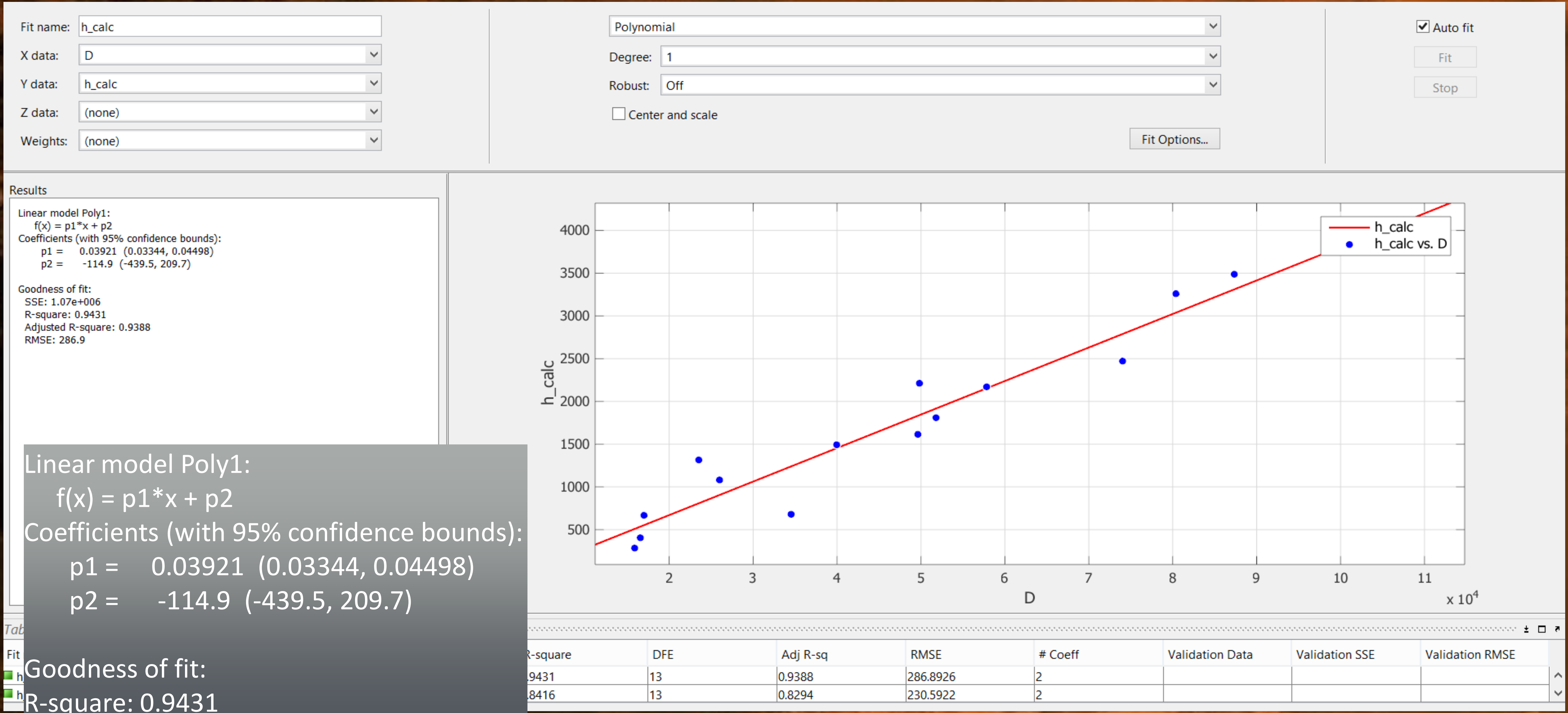

Linear model Poly1:

f(x) = p1*x + p2

Coefficients (with 95% confidence bounds):

p1 = 0.03921 (0.03344, 0.04498)

p2 = -114.9 (-439.5, 209.7)

Goodness of fit:

R-square: 0.9431

linear relationship (as expected)

Step 4: distinction into classes

Therafter we divided craters into classes, using bulge feautures as parameter. We identified three classes, from A to C, possibly showing an evolving process, with A class which represents the most advanced stage.

A Class

Width (m)

Depth (m)

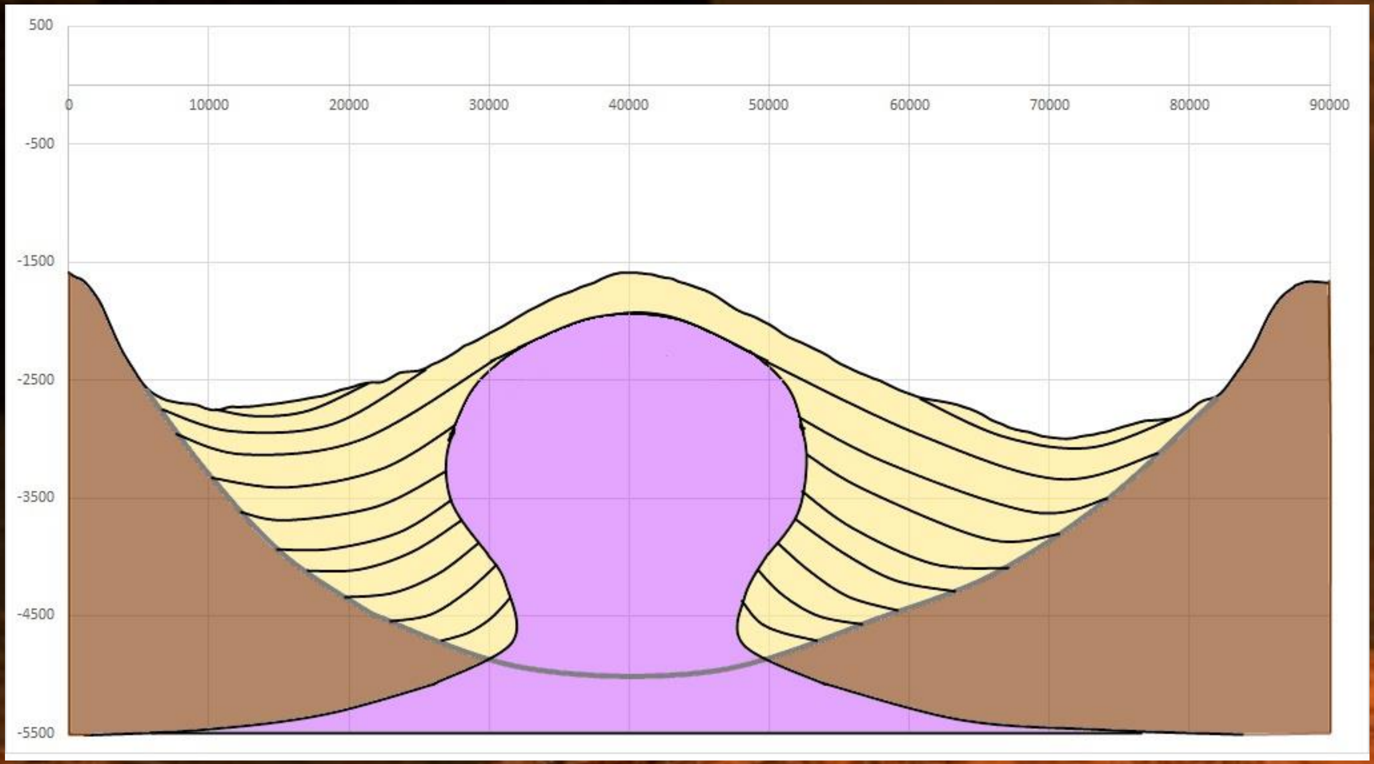

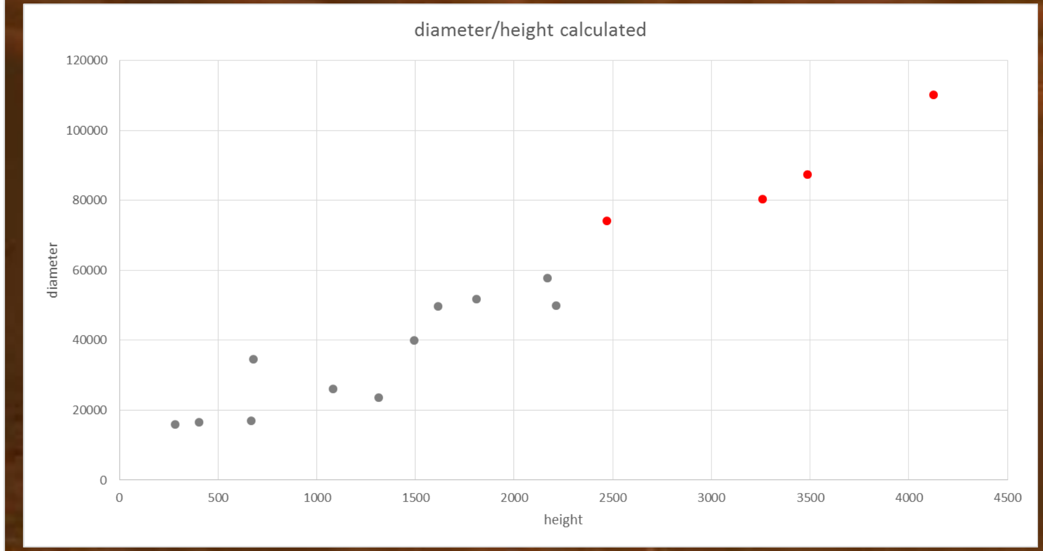

Step 4: distinction into classes

Features: folds, mud volcanoes, centrifugal strata dip directions, high slope angles (30°-45°)

A Class

Width (m)

Depth (m)

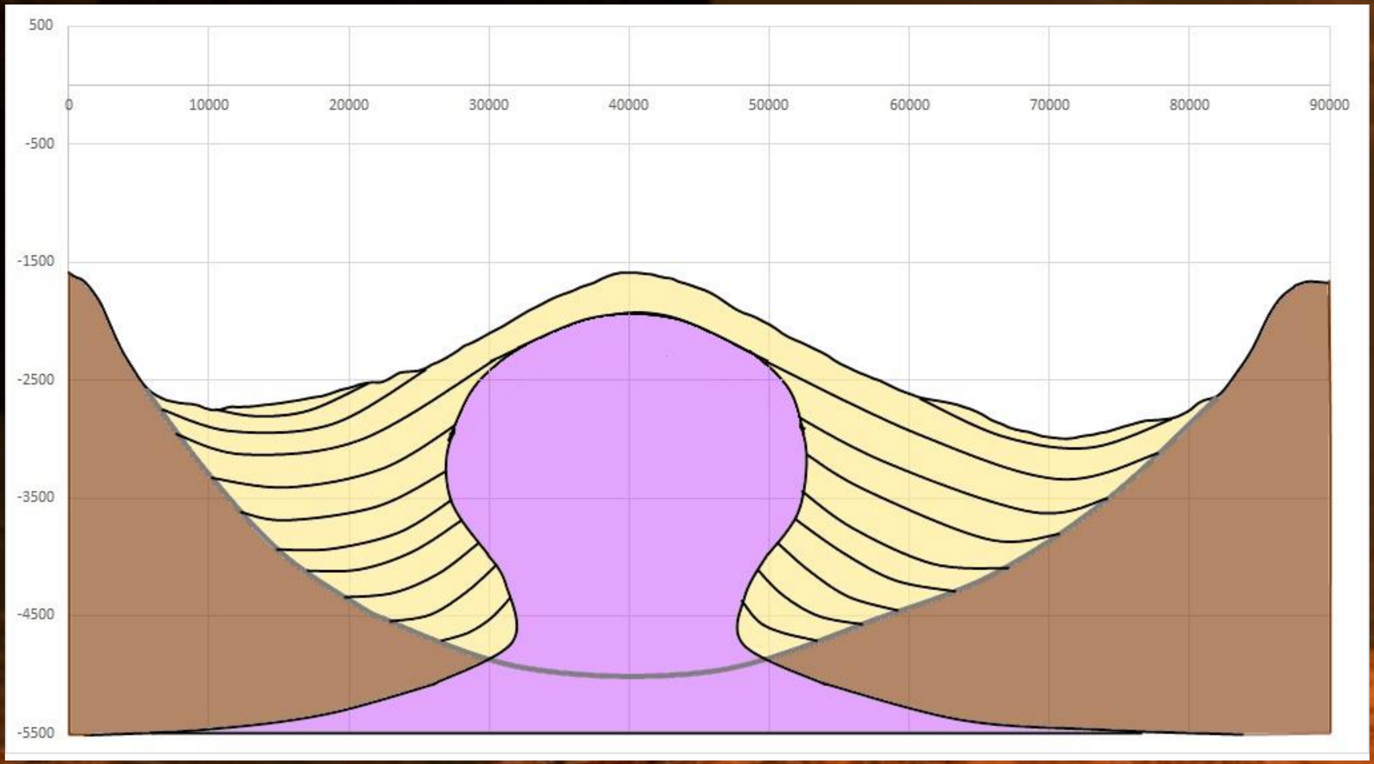

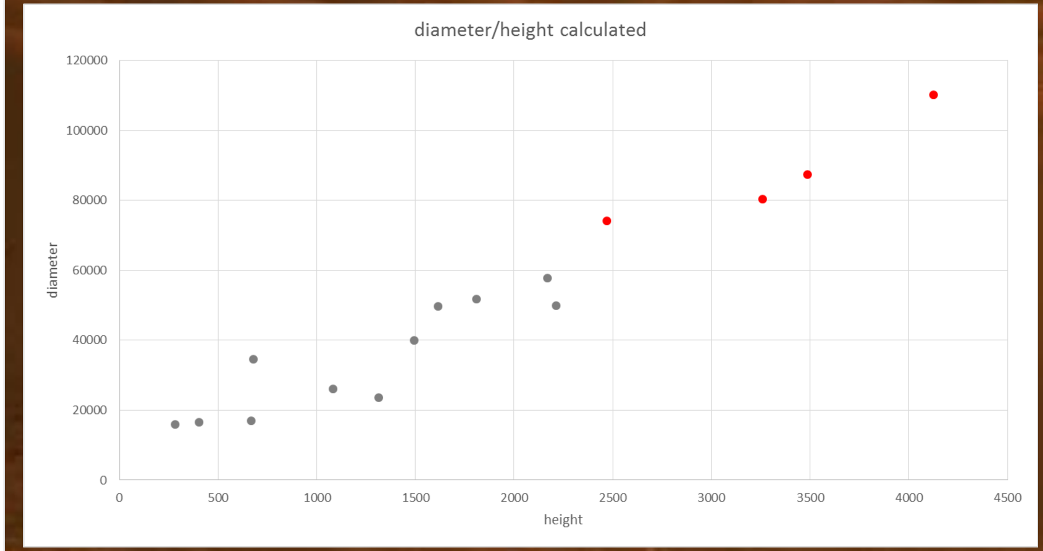

Step 4: distinction into classes

Features: mud volcanoes, centrifugal strata dip directions, intermediate slope angles (≤30°), sinkholes

B Class

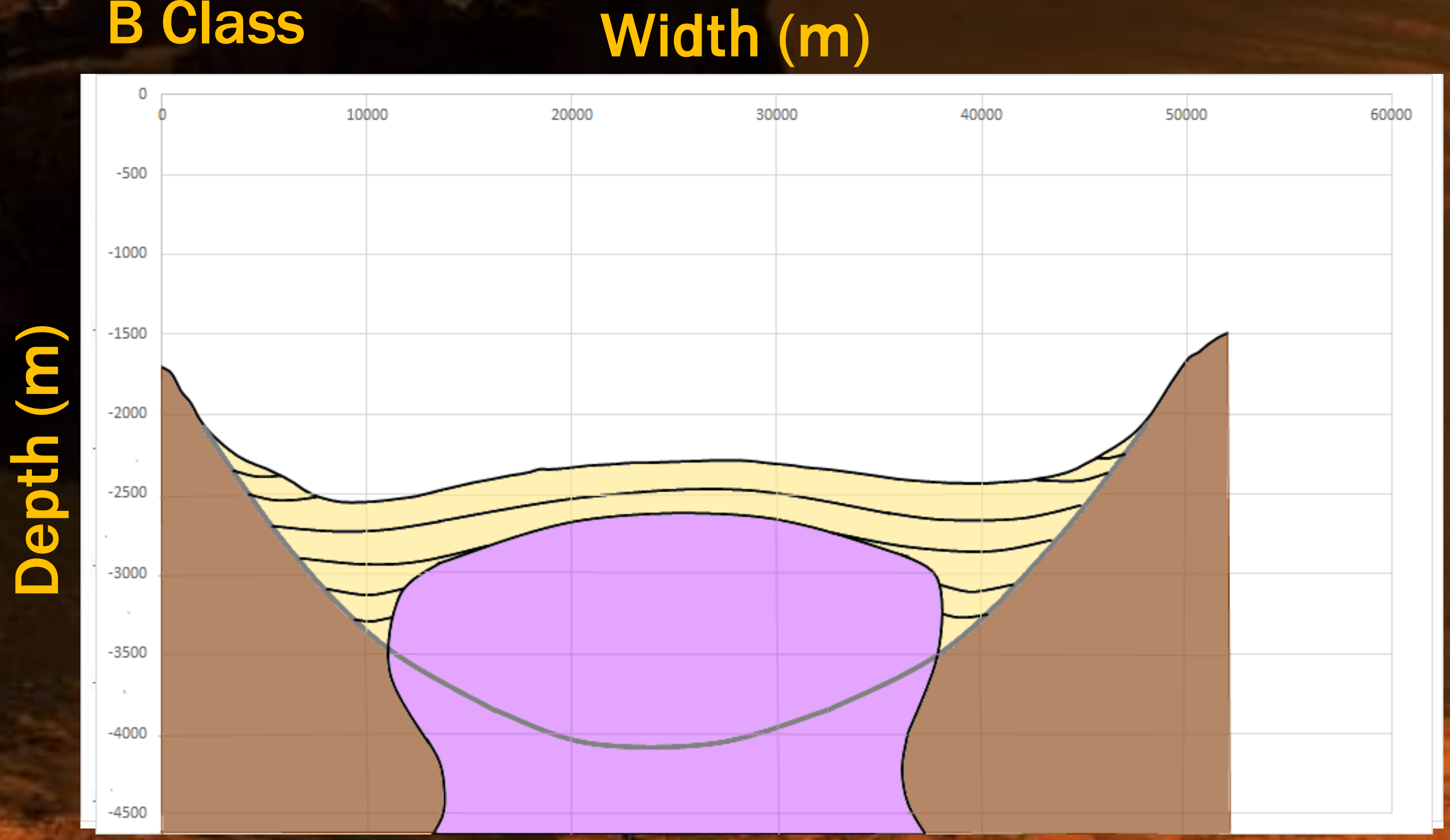

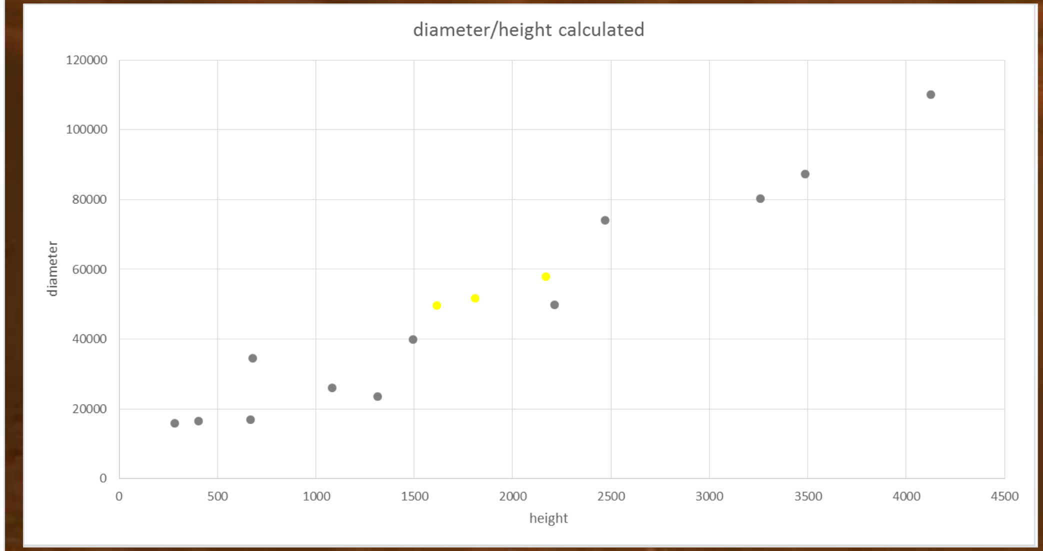

Step 4: distinction into classes

Features: slight bulge with low slope angles (<<30°)

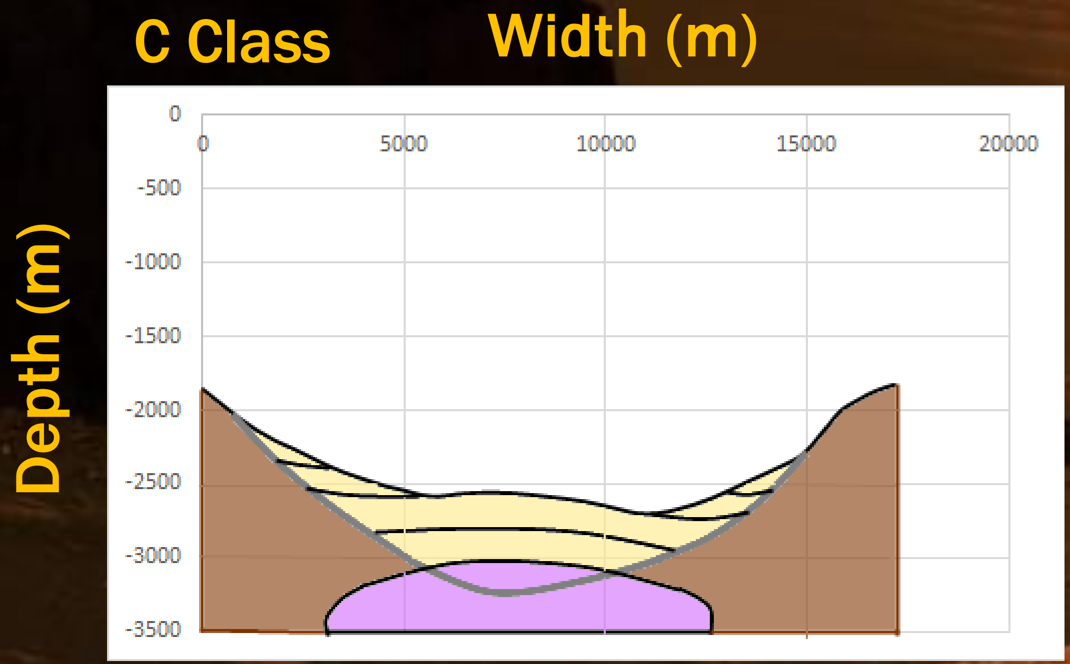

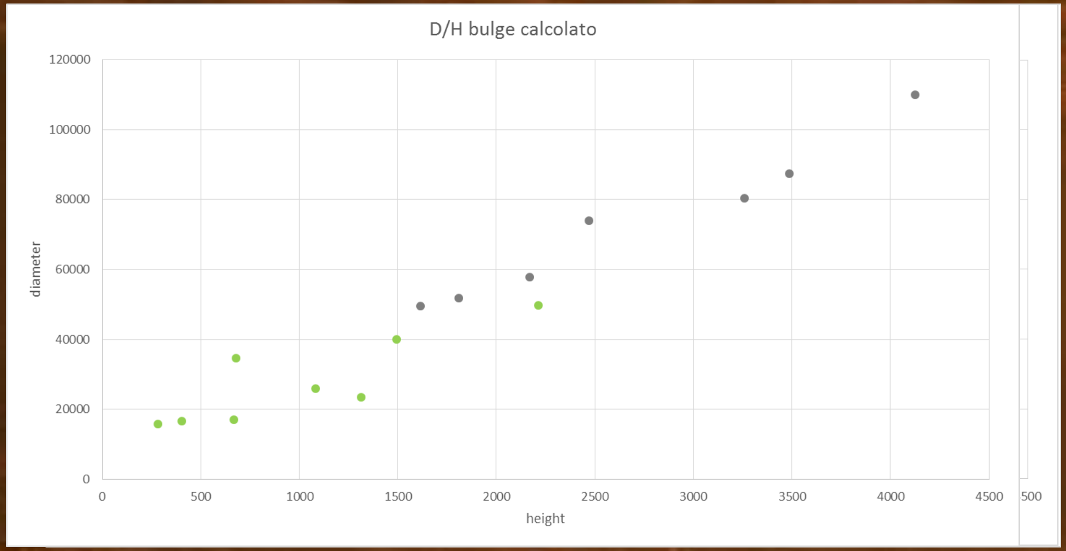

Step 4: distinction into classes

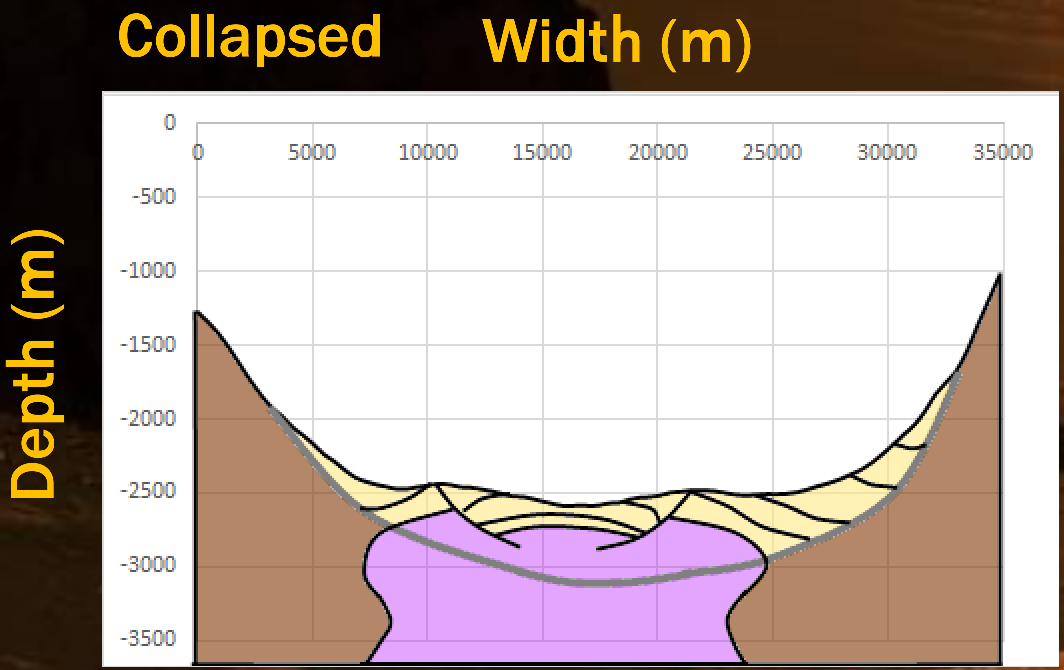

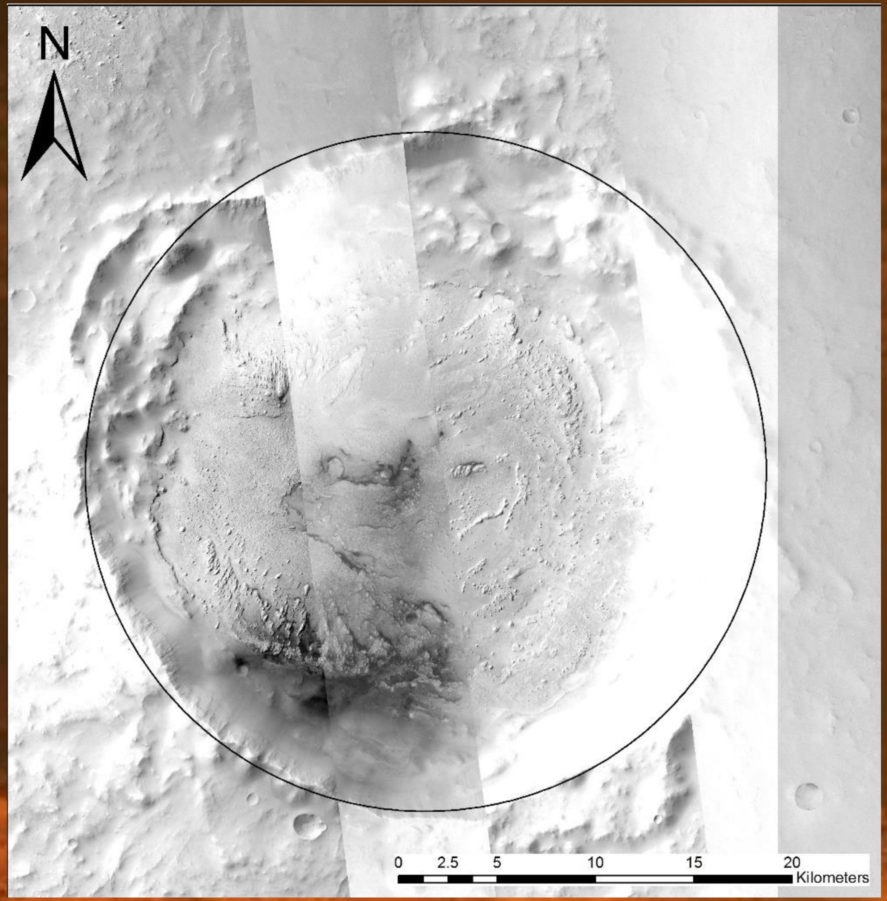

Phase 2: geological mapping of 12000088 crater

It belongs to B class craters. Actually it is composed by two craters which intersect each other.

Data:

- CTX mosaic (6 m/px)
- HiRISE (25 cm/px)
- MOLA (128 px/deg)

Software:

- ArcMap
- ArcCatalog

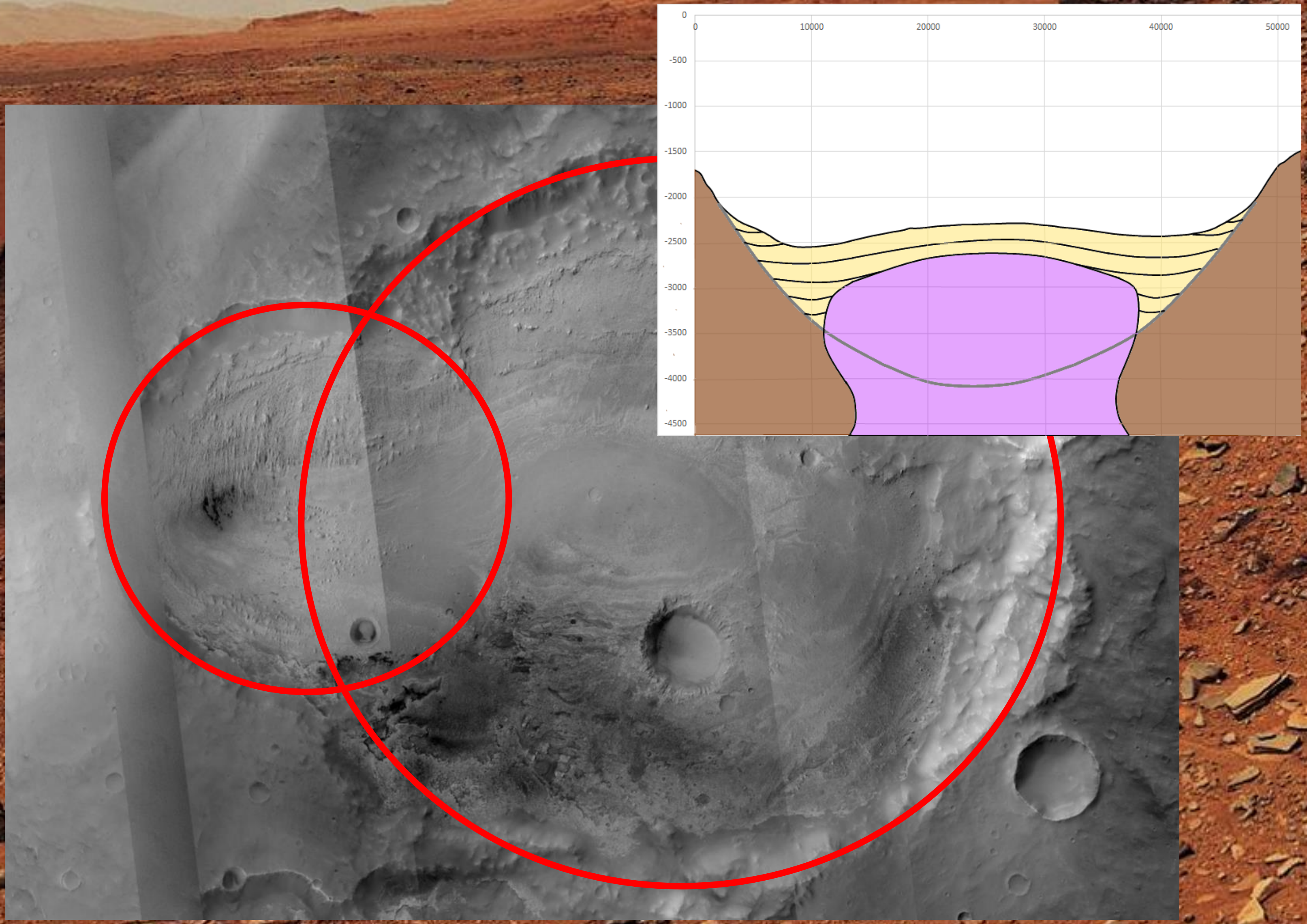

Geological units

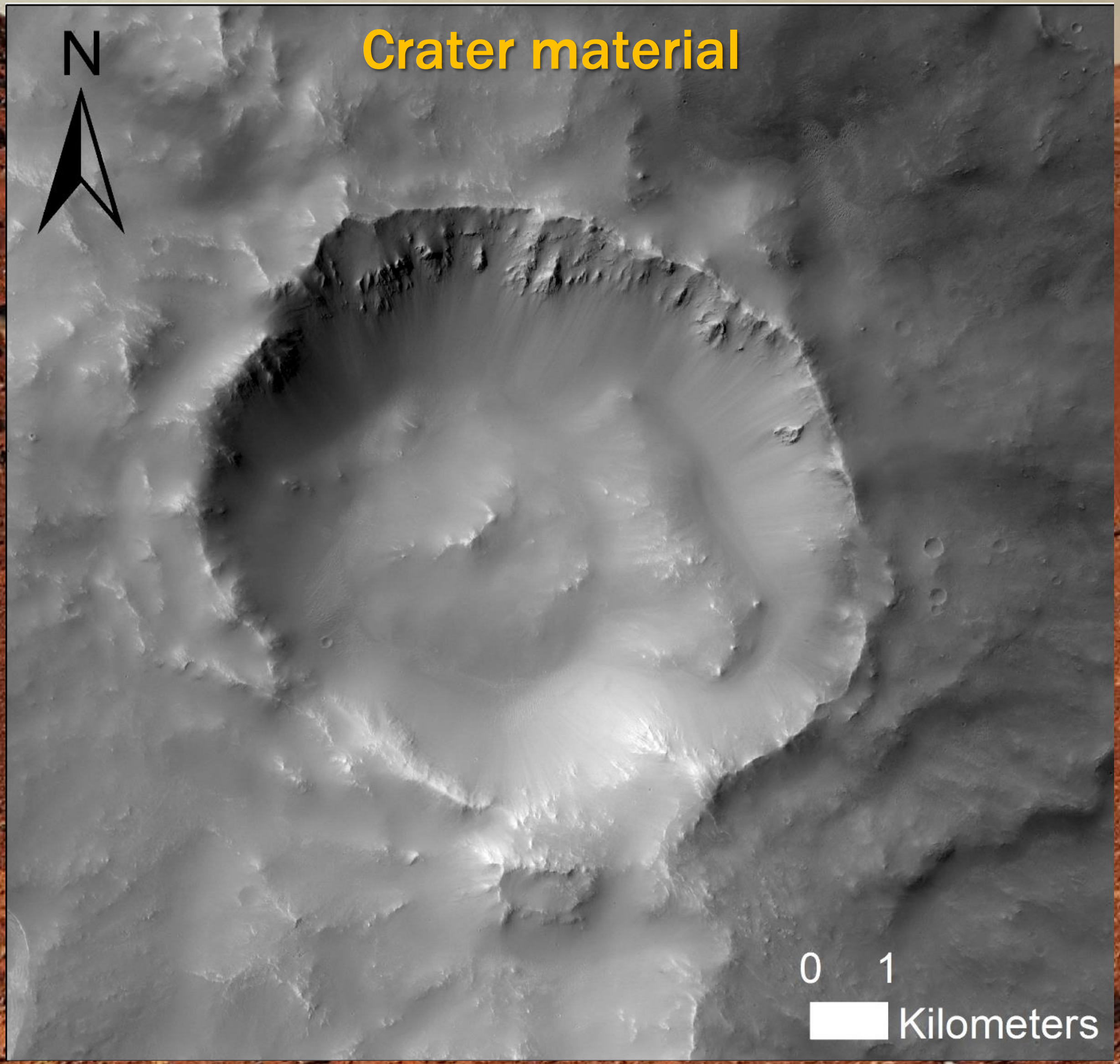

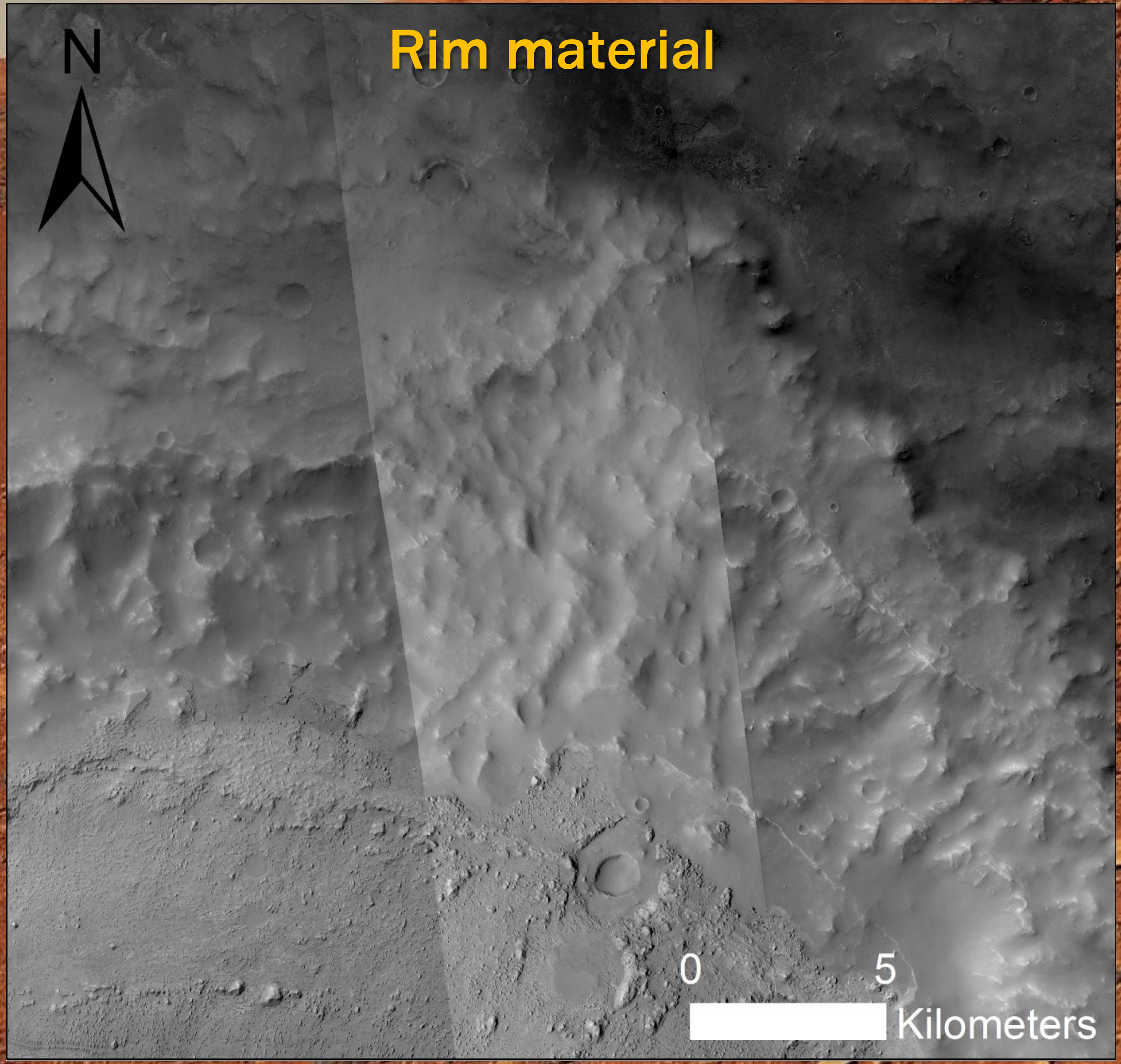

Talus (crater slope)

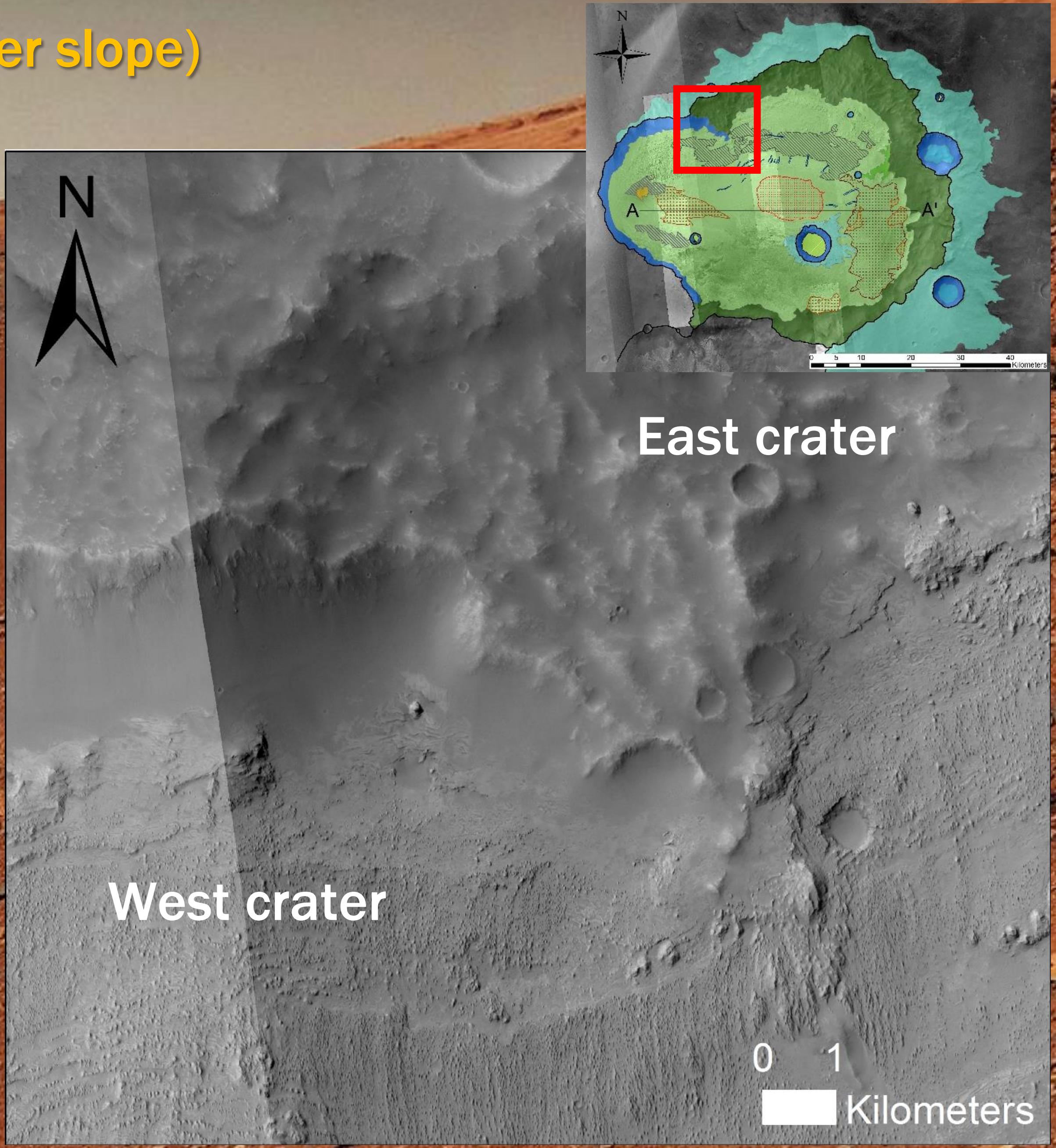

Ejecta

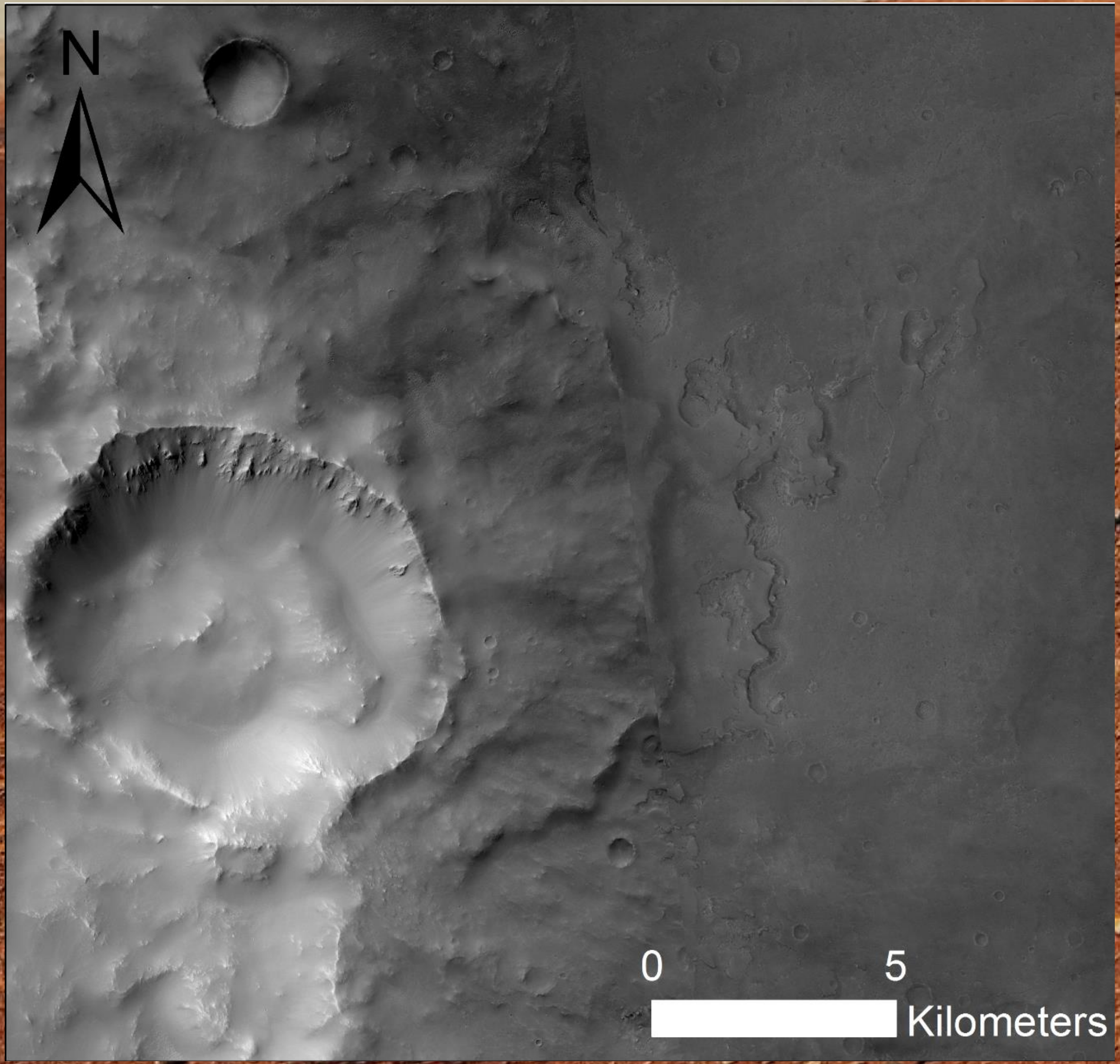

Equatorial Layered Deposits

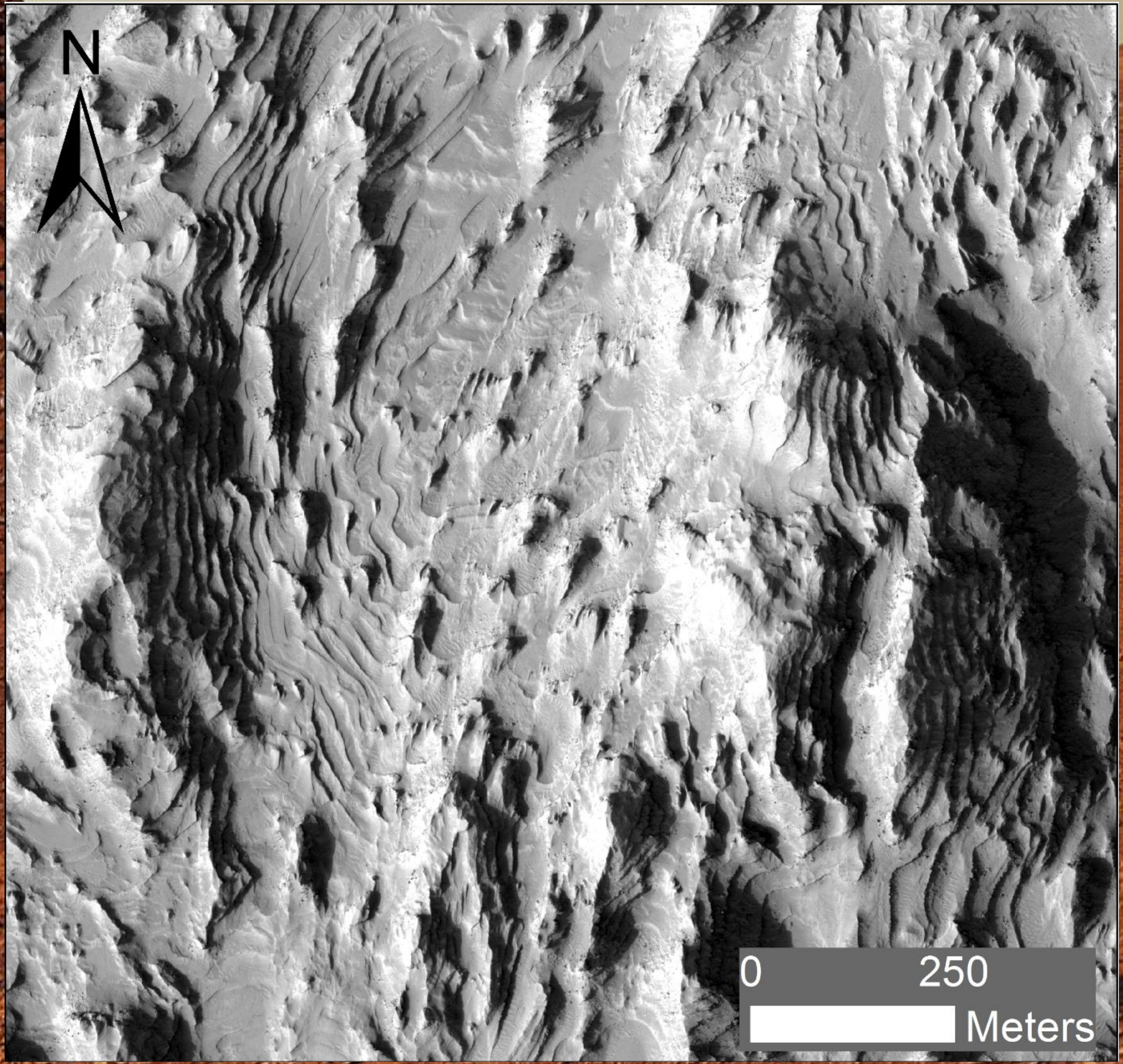

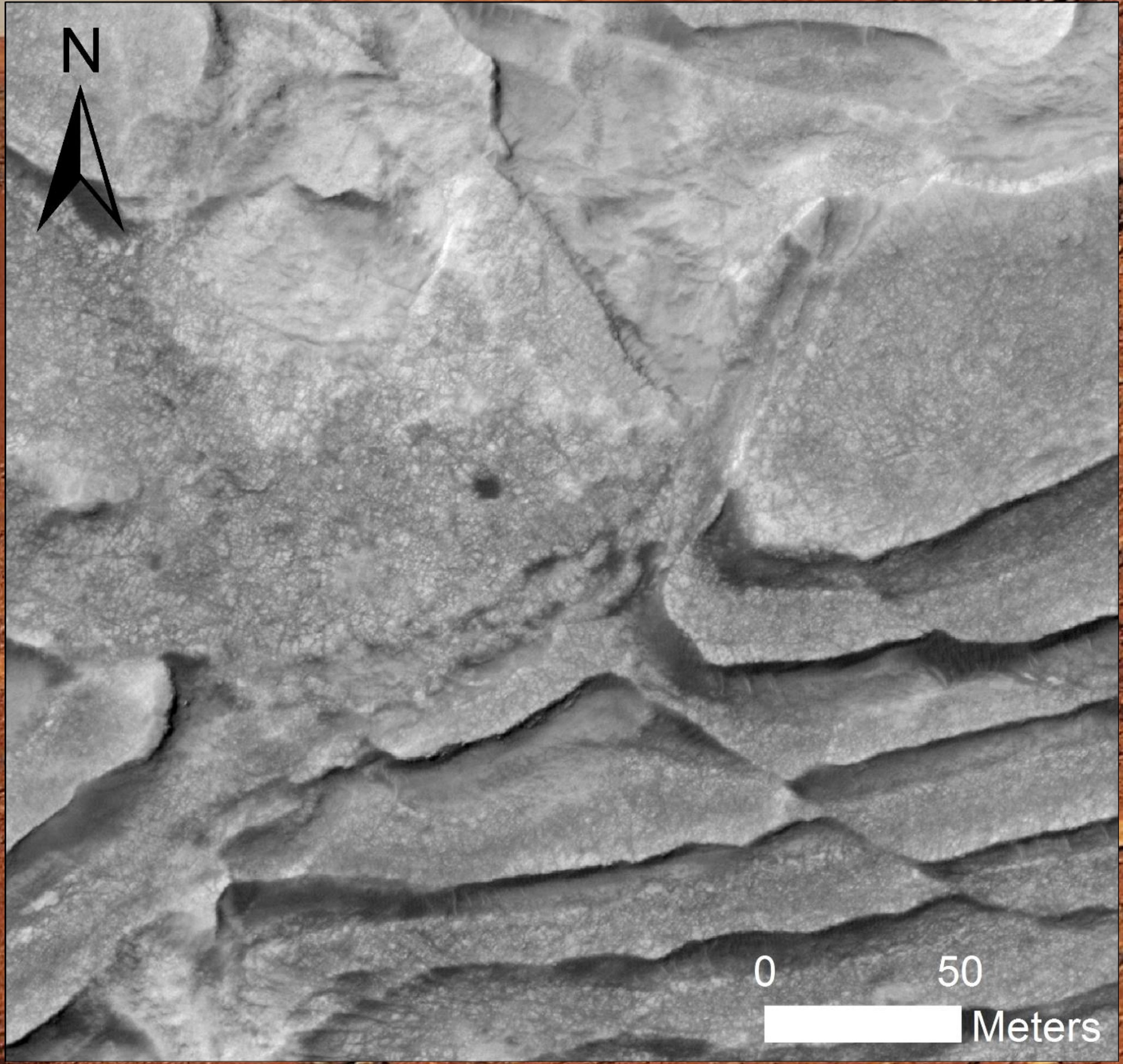

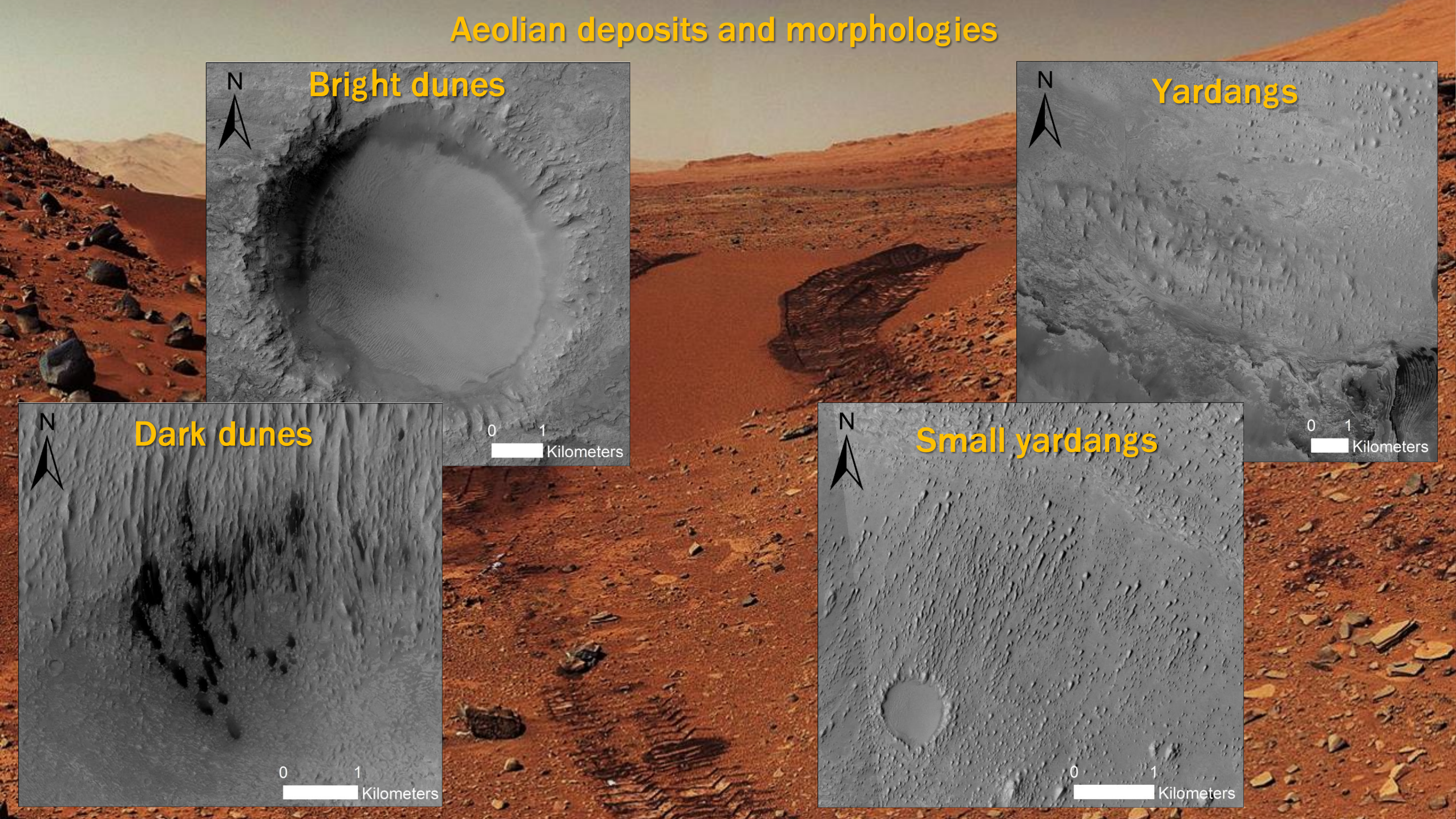

Aeolian deposits and morphologies
Bright dunes
N
0
1
Kilometers
Yardangs
N
0
1
Kilometers
Dark dunes
N
0
1
Kilometers
Small yardangs
N
0
1
Kilometers

Channels

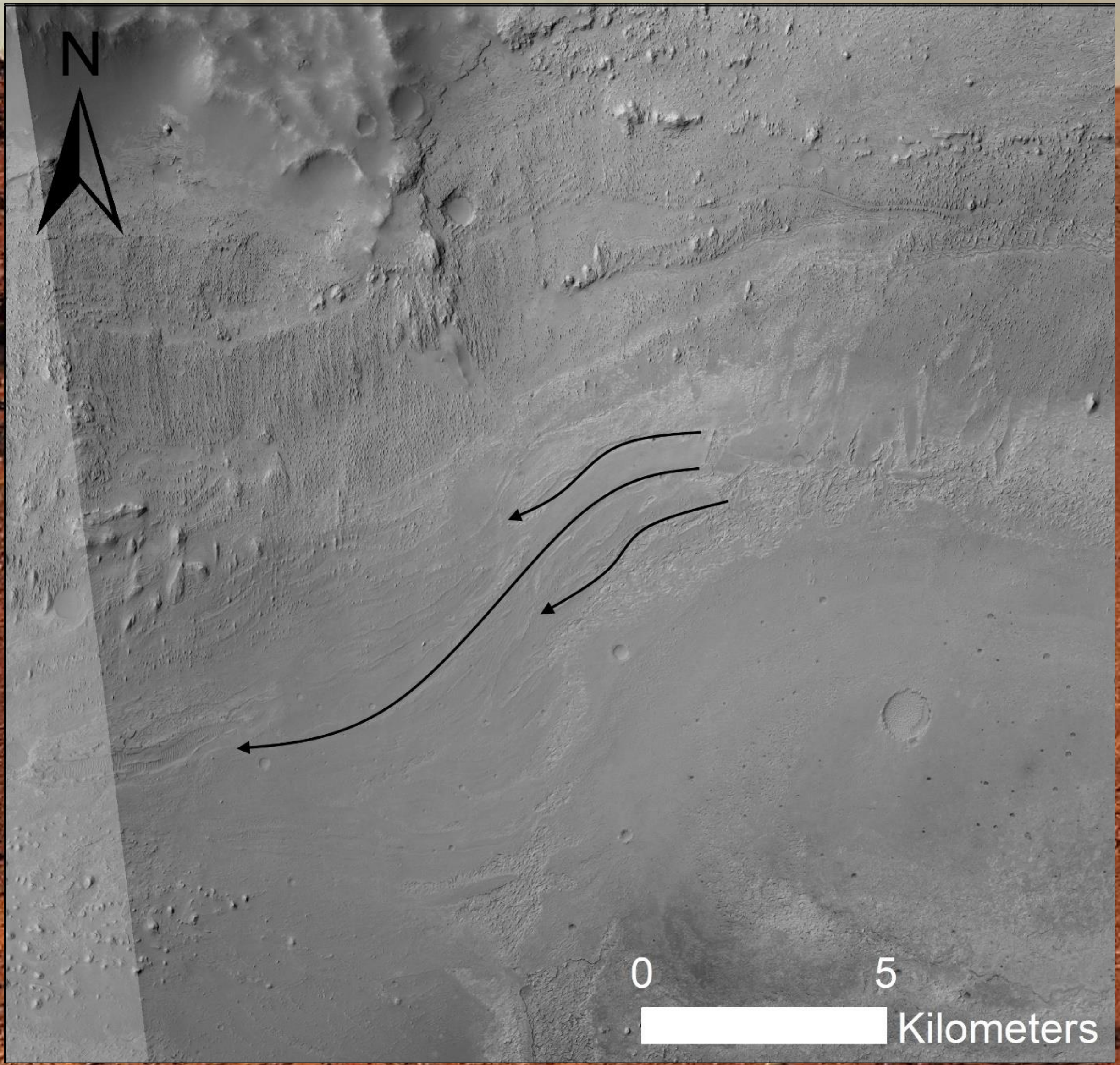
N
0
5
Kilometers

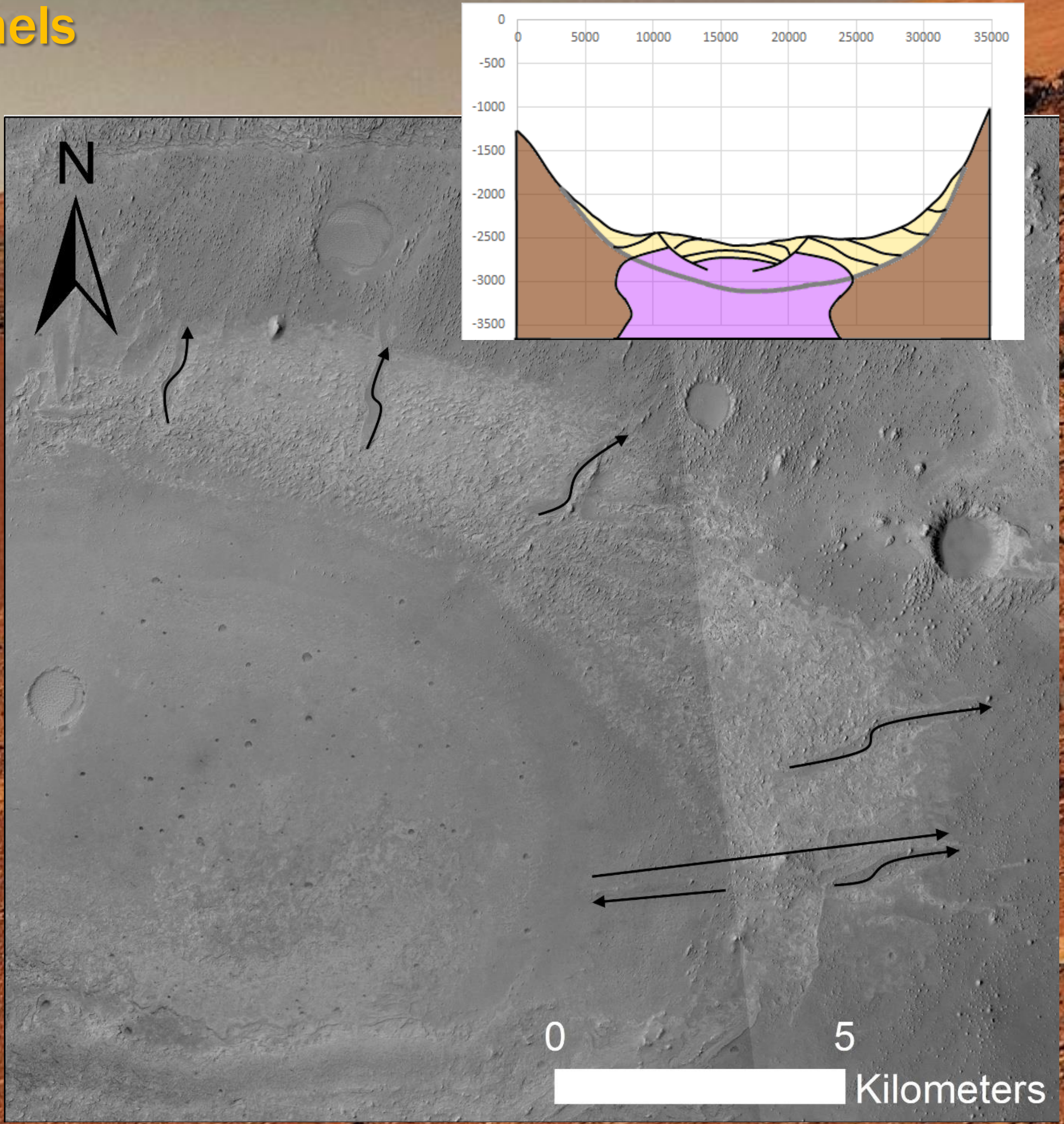
N
0
5
Kilometers
0
5000
10000
15000
20000
25000
30000
35000
0
-500
-1000
-1500
-2000
-2500
-3000
-3500

Sinkholes

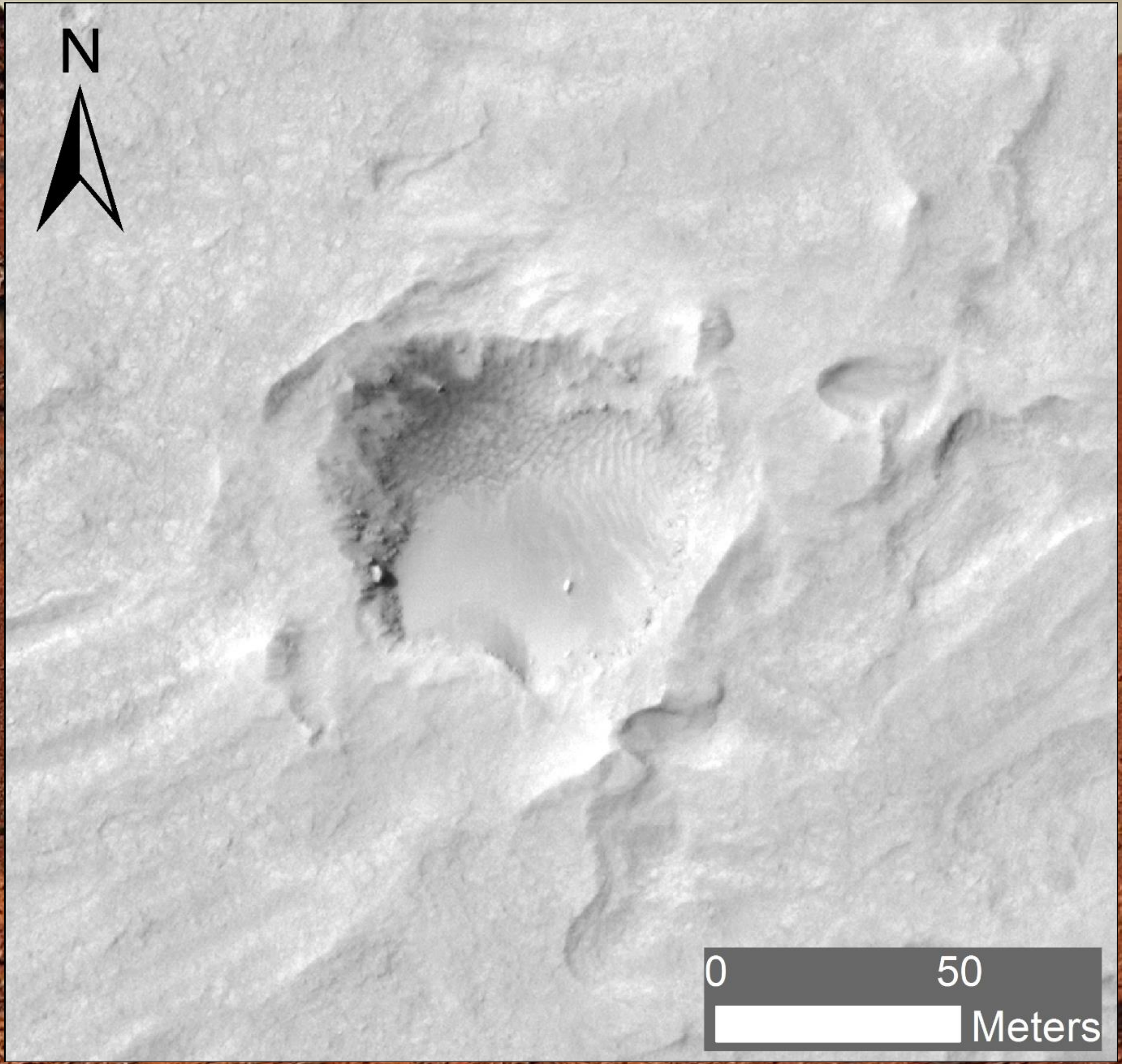

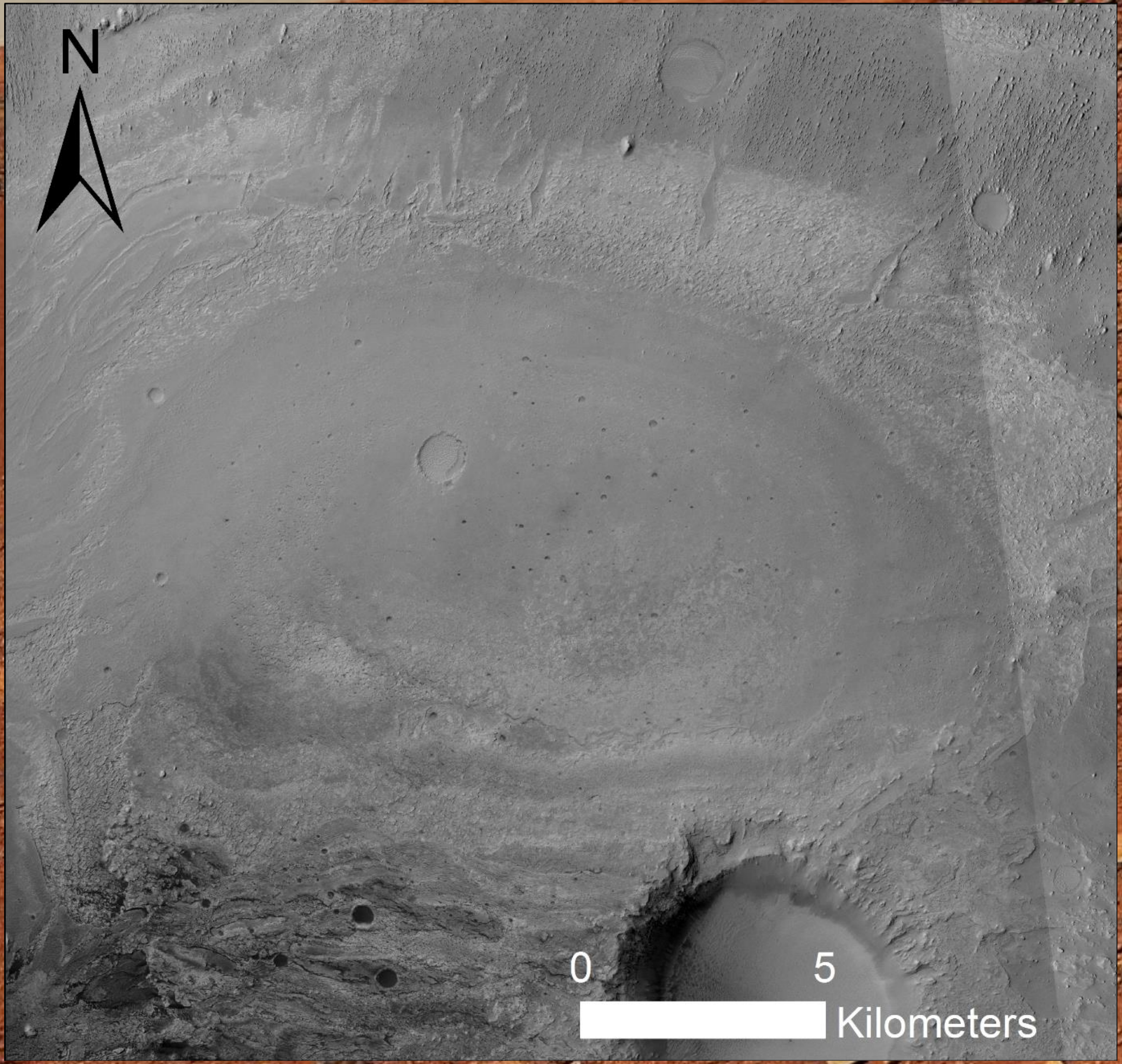

Mounds

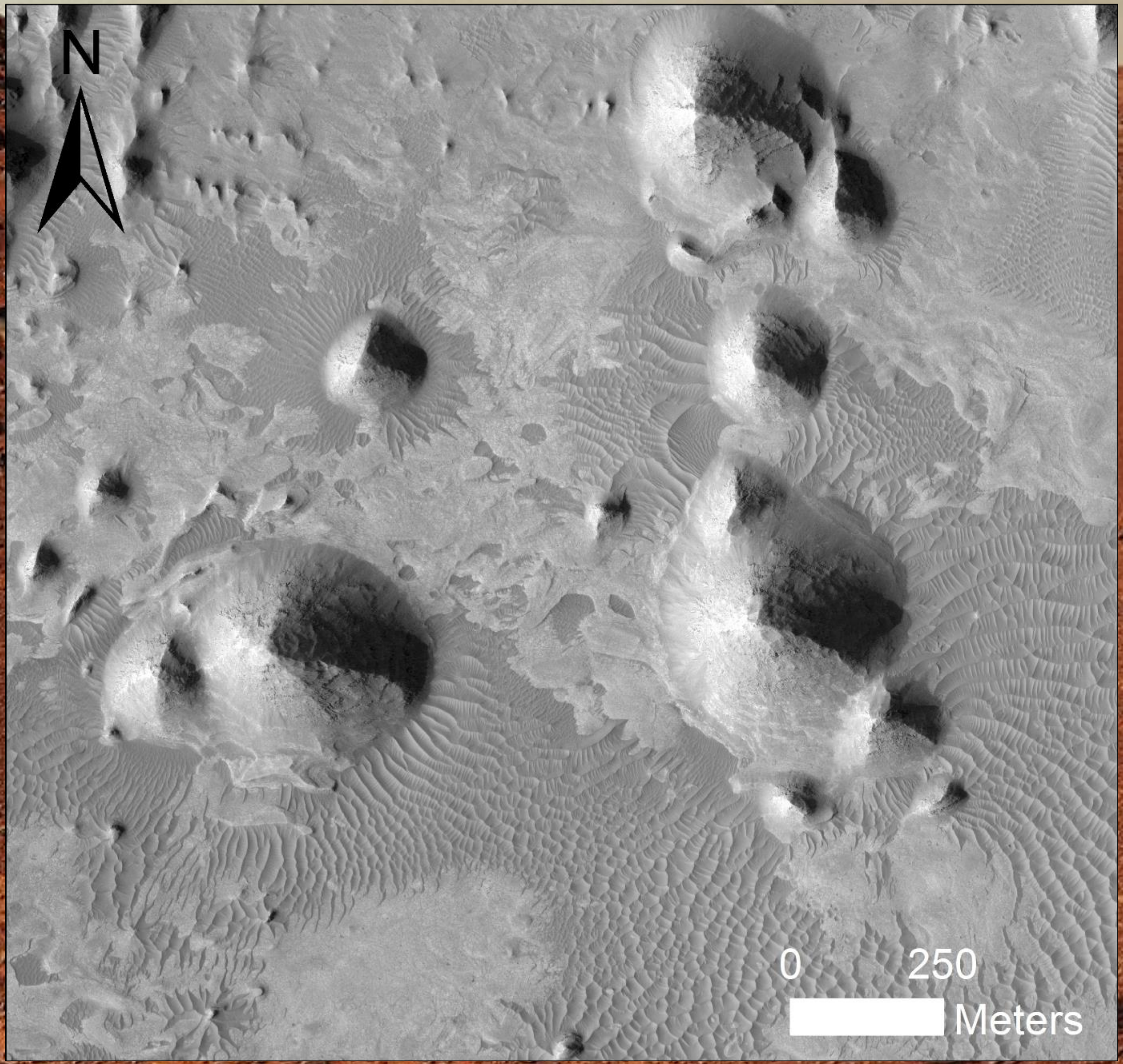

Small mounds

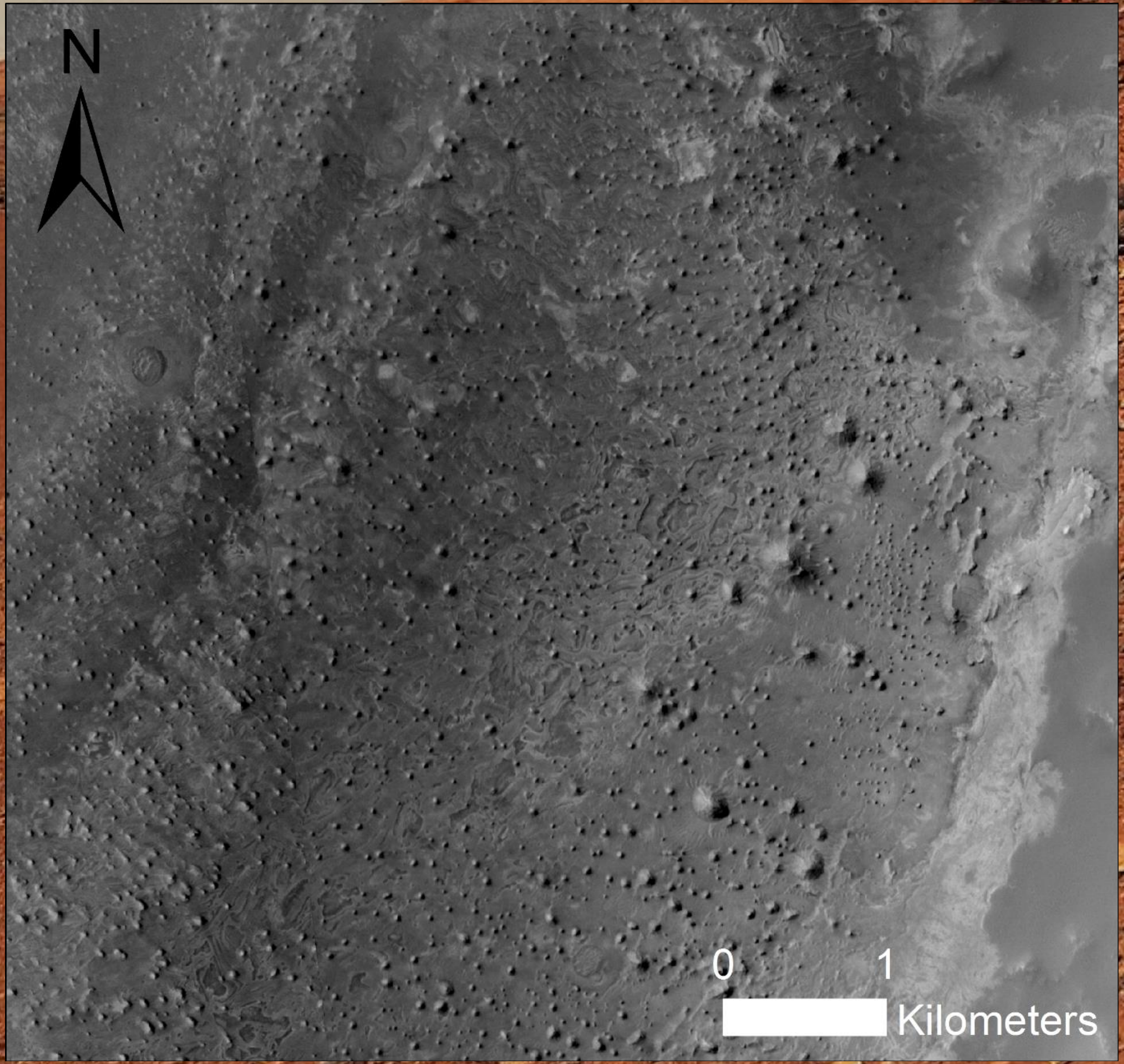

UNIVERSITA' DEGLI STUDI DI PADOVA

GEOLOGICAL MAP OF "12000088" CRATER (ARABIA TERRA, MARS)

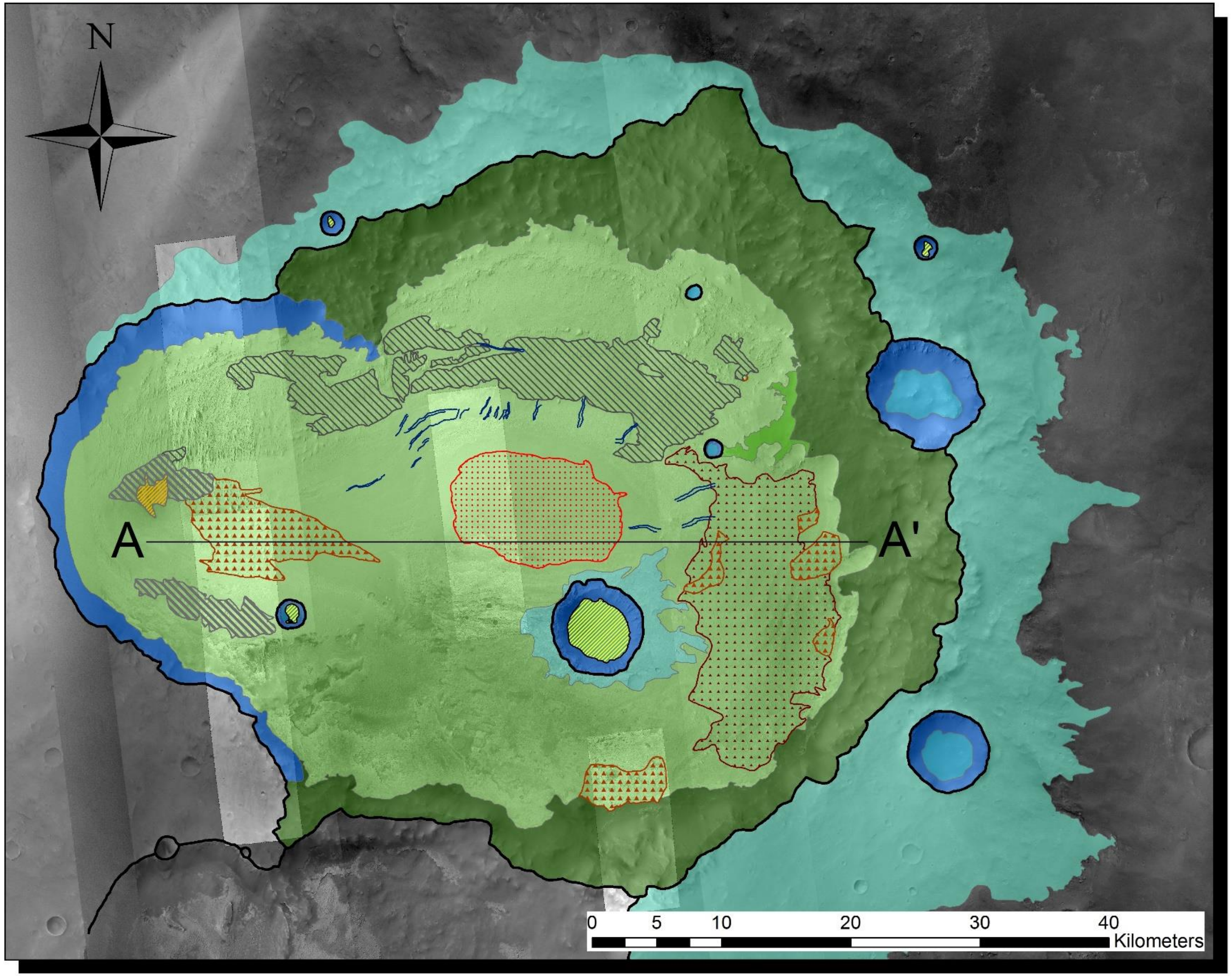

SCALE 1:300000

Legend

- Channel
- Dunes bright
- Dunes dark
- Yardangs
- Yardangs small
- Mounds
- Mounds small
- Sinkholes
- Rim
- Rim material
- Crater material
- Ejecta
- Internal ejecta
- Talus
- Equatorial Layered Deposits

Giovanni Baldo
1027527

UNIVERSITA' DEGLI STUDI DI PADOVA

GEOLOGICAL MAP OF "12000088" CRATER (ARABIA TERRA, MARS)

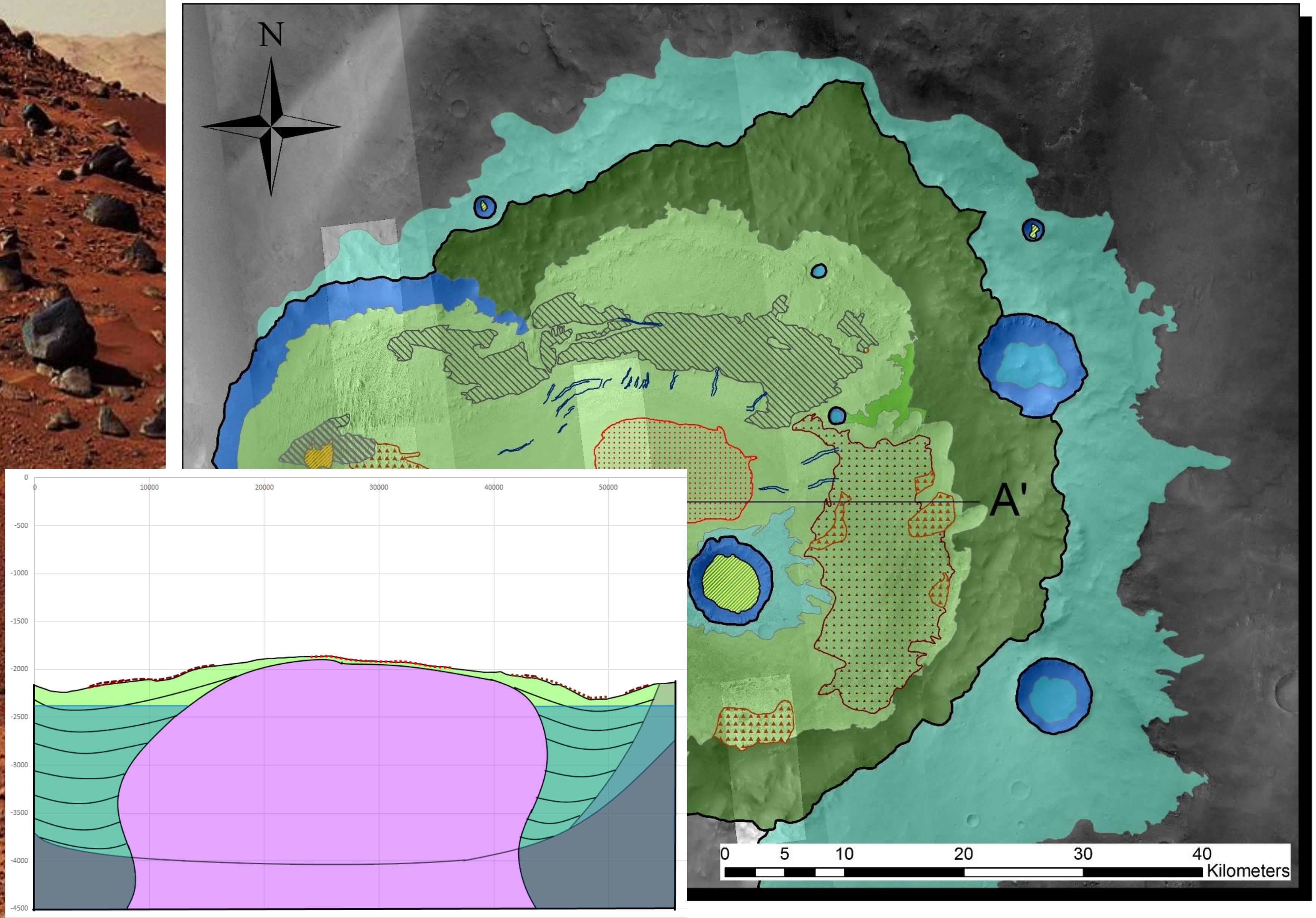

SCALE 1:300000

Legend

- Channel
- Dunes bright
- Dunes dark
- Yardangs
- Yardangs small
- Mounds
- Mounds small
- Sinkholes
- Rim
- Rim material
- Crater material
- Ejecta
- Internal ejecta
- Talus
- Equatorial Layered Deposits

Giovanni Baldo
1027527

Step 5: formation of a bulge

These sketches illustrate the evolution of a bulge. This process began with an impact that created a crater: it caused a differential lithostatic load onto a deep evaporitic layer. The underlying salt stratum used the fractured brittle zone below the crater to flow into a diapir.

Stage one

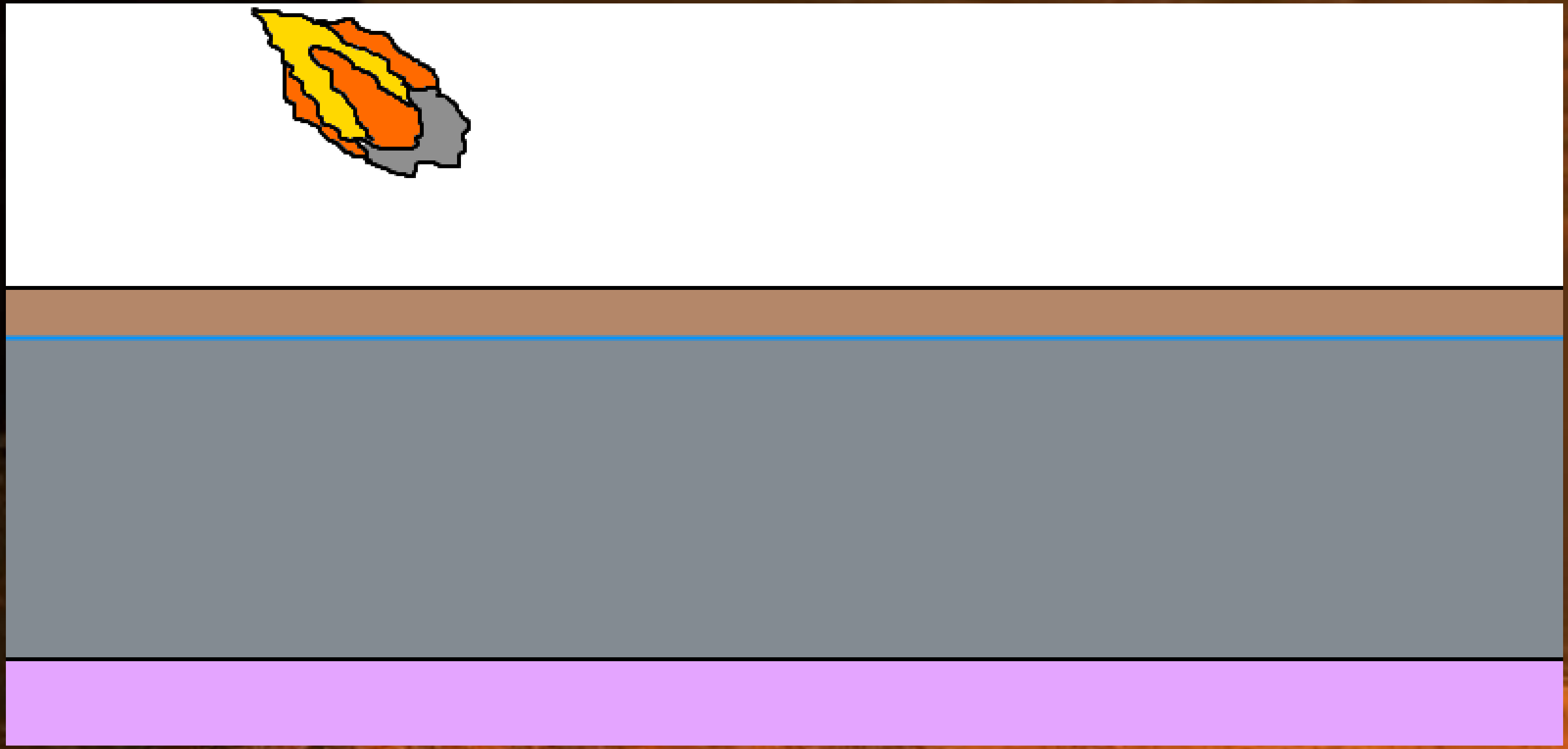

Step 5: formation of a bulge

These sketches illustrate the evolution of a bulge. This process began with an impact that created a crater: it caused a differential lithostatic load onto a deep evaporitic layer. The underlying salt stratum used the fractured brittle zone below the crater to flow into a diapir.

Stage two

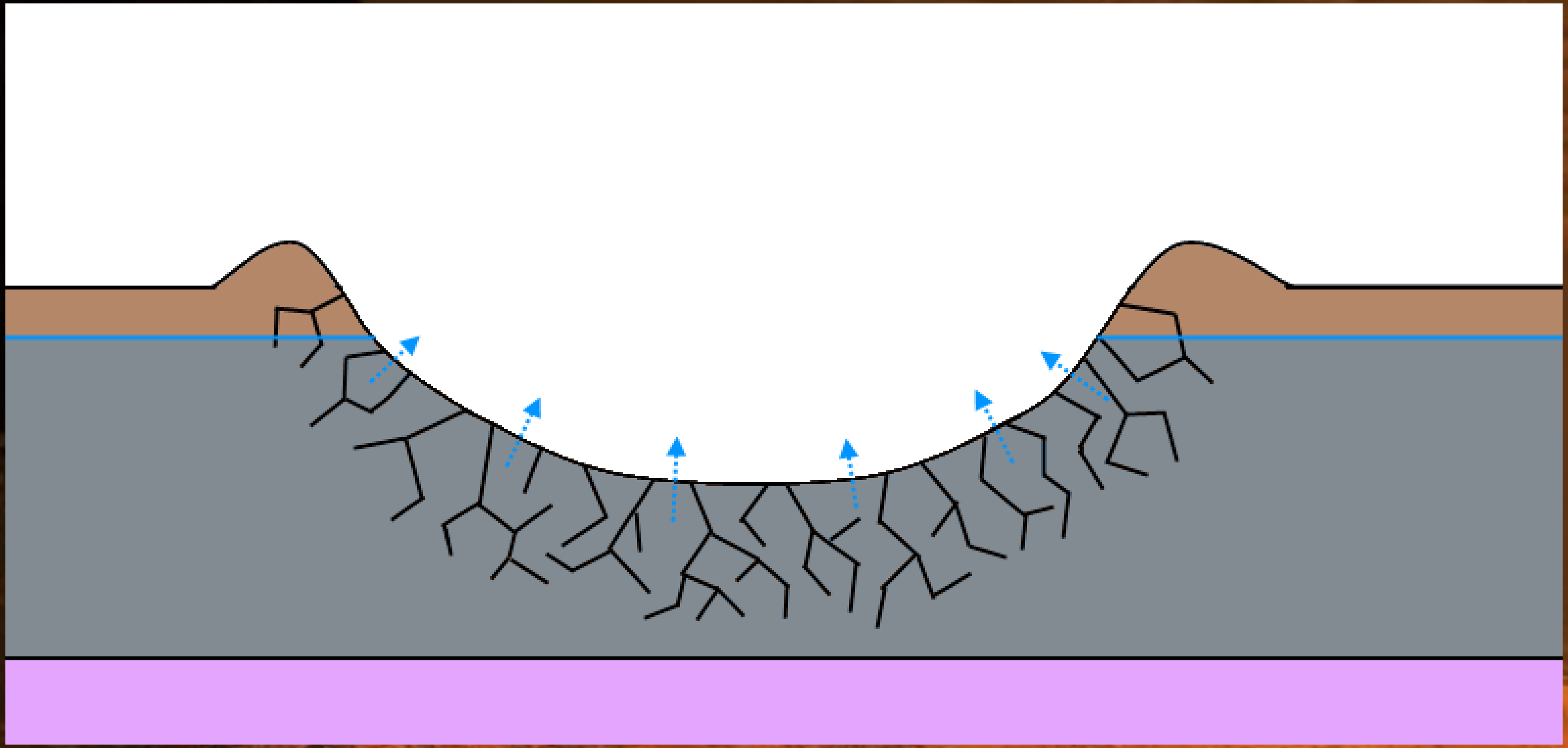

Step 5: formation of a bulge

These sketches illustrate the evolution of a bulge. This process began with an impact that created a crater: it caused a differential lithostatic load onto a deep evaporitic layer. The underlying salt stratum used the fractured brittle zone below the crater to flow into a diapir.

Stage two

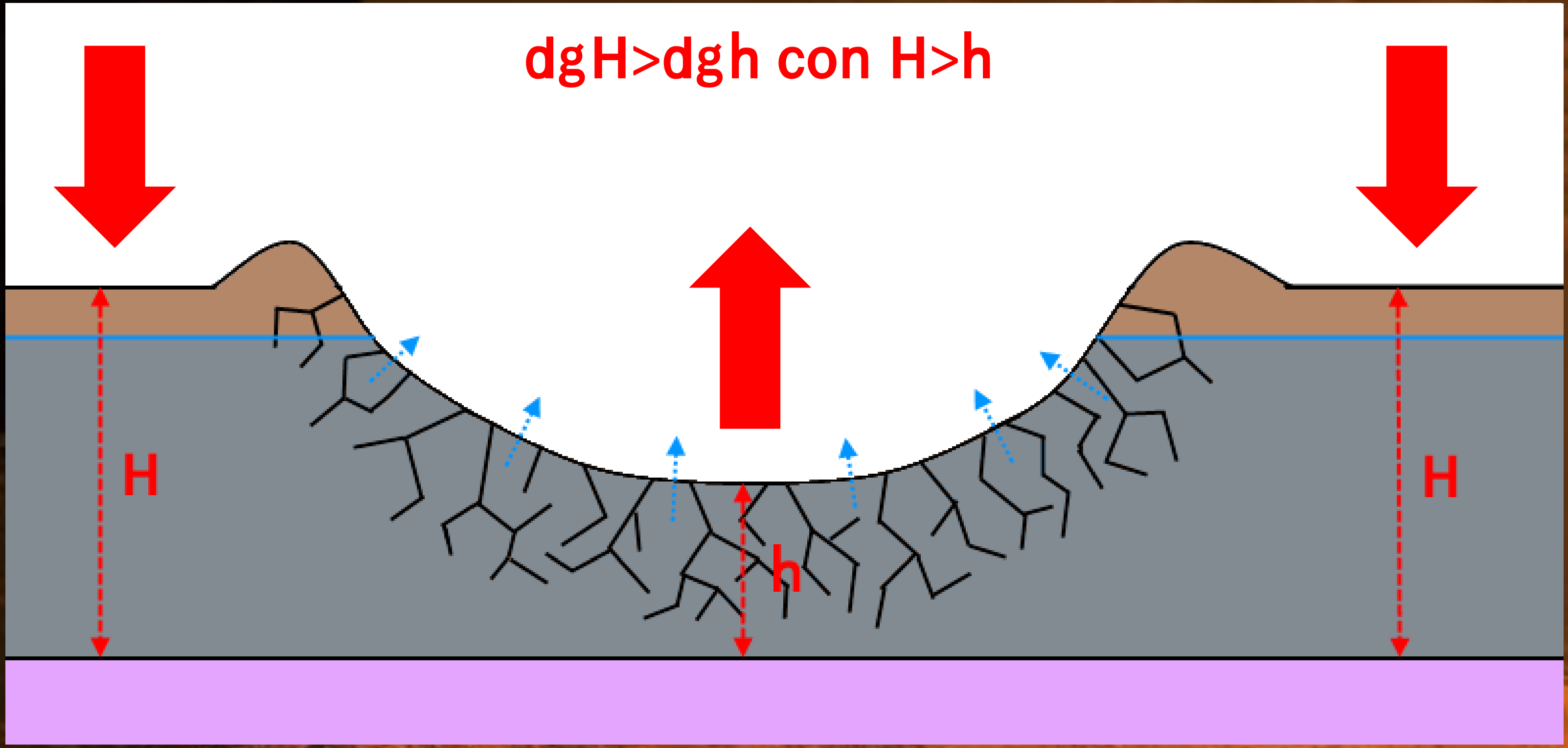

Step 5: formation of a bulge

These sketches illustrate the evolution of a bulge. This process began with an impact that created a crater: it caused a differential lithostatic load. The underlying salt stratum used the fractured brittle zone below the crater to flow into a diapir.

Stage three

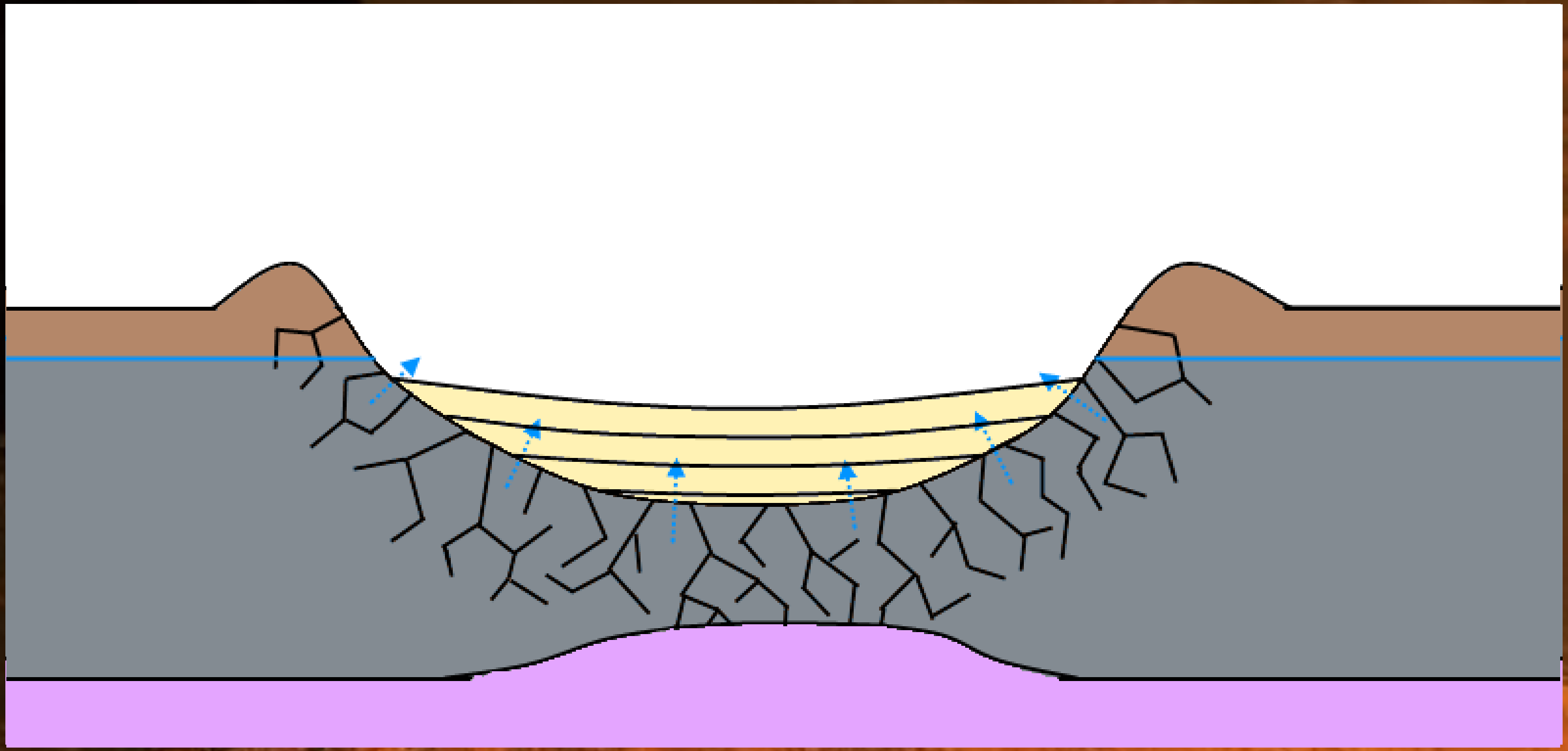

Step 5: formation of a bulge

These sketches illustrate the evolution of a bulge. This process began with an impact that created a crater: it caused a differential lithostatic load onto a deep evaporitic layer. The underlying salt stratum used the fractured brittle zone below the crater to flow into a diapir.

Stage four

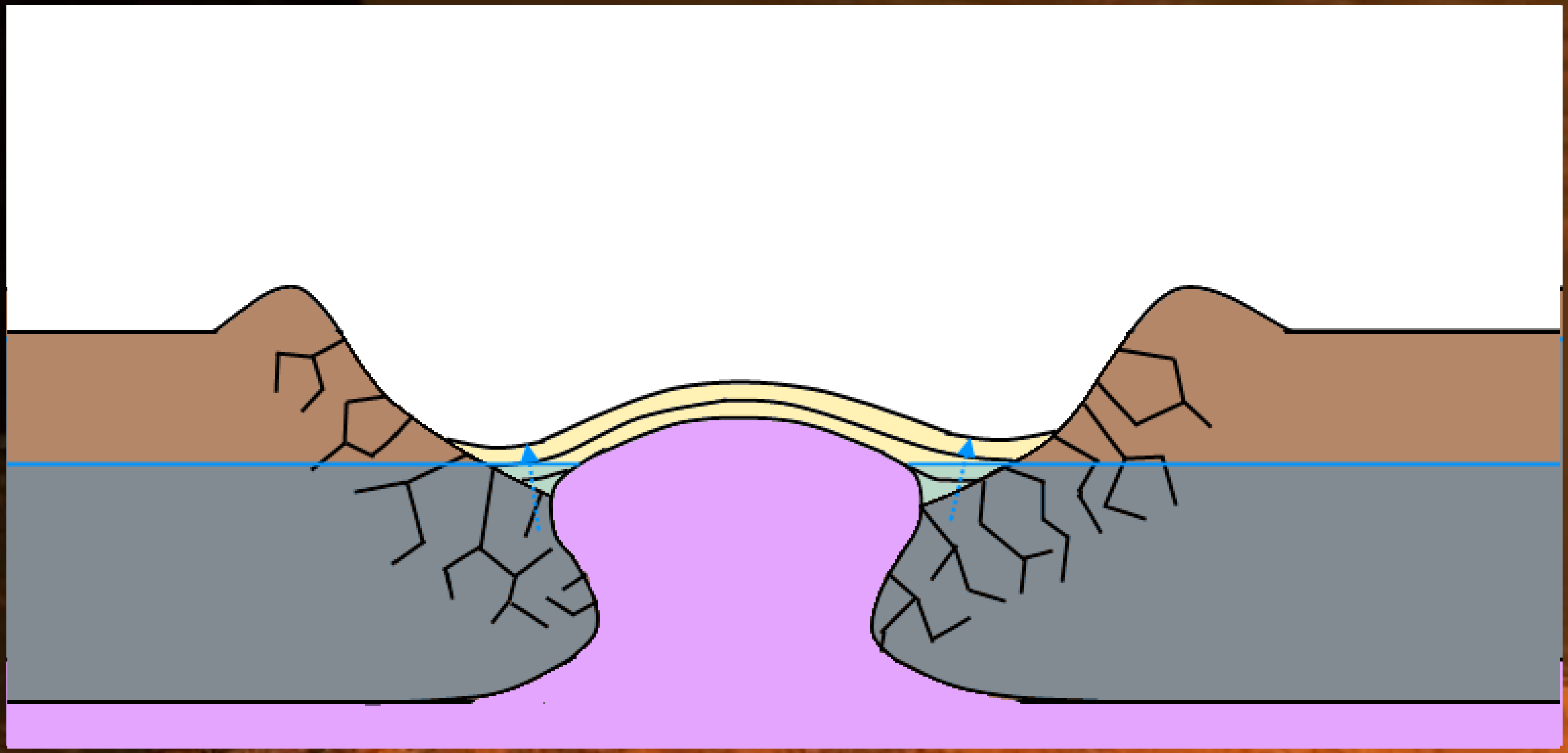

Conclusions

Finally, following our analysis, we have reached two important results:

- We have discovered the presence of a connection which tie up the craters diameter with the height of the bulge, both in the relationship with measured data and in the one with calculated data (found through the Robbins equation).

- We have observed, as a consequence of the cataloguing of all the craters which show a bulge and of the geological analysis of one of them, the presence of different features wich suggest us the exsistence of an upwelling evaporitic body.